Centrum voor Wiskunde en Informatica
Centre for Mathematics and Computer Science

P.M. de Zeeuw

Nonlinear multigrid applied to a
1D stationary semiconductor model

Department of Numerical Mathematics Report NM-R8905 February

The Centre for Mathematics and Computer Science is a research institute of the Stichting Mathematisch Centrum, which was founded on February 11, 1946, as a nonprofit institution aiming at the promotion of mathematics, computer science, and their applications. It is sponsored by the Dutch Government through the Netherlands Organization for the Advancement of Research (N.W.O.).

Nonlinear Multigrid applied to a 1D Stationary Semiconductor Model

P.M. de Zeeuw
Centre for Mathematics and Computer Science
P.O. Box 4079, 1009 AB Amsterdam, The Netherlands

The nonlinear multigrid method is applied to a transistor problem in one dimension. A weak spot in the linearization of the well-known Scharfetter-Gummel discretization scheme is reported. Further it is shown that both the residual transfer and the solution transfer from a fine to a coarse grid need special requirements due to the rapidly varying problem coefficients. Some modifications are proposed which make the multigrid algorithm perform well for the hard example problem.

1980 Mathematics Subject Classification: 65N20, 65H10.
Key Words and Phrases: semiconductor equations, multigrid methods.

1. Introduction

There is a great demand for a proper numerical simulation of semiconductors in order to reduce the costs of constructing expensive prototypes. The search for a fast and robust algorithm has proven to be a challenge. So far only a few papers have considered the multigrid solution of the discrete semiconductor equations (e.g. cf. [1,2,4,7,9]) and therefore extensive further research is required.

In this paper we restrict ourselves on purpose to one space dimension as a preparatory study for the case of more space dimensions. We study a particular example problem which has been put forward by Dr. W.H.A. Schilders, Philips; the Netherlands. This problem models a transistor and turns out to be a lot harder to solve than the forward or reversed biased diode problem. We apply nonlinear multigrid and encounter a serious difficulty due to the nonlinearity of the problem. The difficulty is analysed and this undoubtedly provides insight equally well for the case of more spacedimensions. Some modifications are proposed which significantly increase the robustness of the nonlinear multigrid method and which look promising also for the more-dimensional case.

2. The problem

The behaviour of a steady semiconductor device can be described by the following set of equations (cf. [8]):

$$\nabla(-\epsilon\nabla\psi) = q(p-n+D), \tag{2.1a}$$

$$\nabla J_n = +qR, \tag{2.1b}$$

$$\nabla J_p = -qR, \tag{2.1c}$$

where J_n and J_p are defined by

$$J_n = q\mu_n(\frac{1}{\alpha}\nabla n - n\nabla\psi), \tag{2.2a}$$

$$J_p = -q\mu_p(\frac{1}{\alpha}\nabla p + p\nabla\psi). \tag{2.2b}$$

Substitution of (2.2) into (2.1) results in a system of three nonlinear partial differential equations for ψ,n and p. In (2.1) ψ represents the electrostatic potential, p and n describe the concentration of holes and electrons respectively. Equations (2.1b) and (2.1c) are called the continuity equations; J_n is the

Report NM-R8905
Centre for Mathematics and Computer Science
P.O. Box 4079, 1009 AB Amsterdam, The Netherlands

electron current density, J_p is the hole current density, R is the recombination-generation rate, a function of n and p. The doping profile D is a function of the space variable x. The quantities $\epsilon, q, \alpha, \mu_n, \mu_p$ represent the permittivity, the elementary charge, the inverse of the thermal voltage and the electron and hole mobility respectively.

In this paper we consider the case of only one space dimension and assume ϵ, α, μ_n and μ_p to be constant. It is common practice to replace the variables n and p by the hole and electron quasi-Fermi potentials ϕ_n and ϕ_p defined by the relations:

$$n = n_i e^{\alpha(\psi - \phi_n)}, \tag{2.3a}$$

$$p = n_i e^{\alpha(\phi_p - \psi)}. \tag{2.3b}$$

On the one hand, by this change of variables, the nonlinearity of the problem is strongly increased, on the other hand the values assumed by (ψ, ϕ_n, ϕ_p) are in a much more moderate range. For extensive discussions on the choice of variables cf. [7,8]. Using (2.3) the equations (2.1) are transformed into

$$-\nabla J_\psi = n_i q(e^{\alpha(\phi_p - \psi)} - e^{\alpha(\psi - \phi_n)}) + qD, \tag{2.4a}$$

$$-\nabla J_n = +qR, \tag{2.4b}$$

$$-\nabla J_p = -qR, \tag{2.4c}$$

where J_ψ is defined by

$$J_\psi = \epsilon \nabla \psi, \tag{2.5a}$$

and J_n, J_p are now defined by

$$J_n = \bar{\mu}_n e^{\alpha(\psi - \phi_n)} \nabla(\alpha \phi_n), \tag{2.5b}$$

$$J_p = \bar{\mu}_p e^{\alpha(\phi_p - \psi)} \nabla(\alpha \phi_p), \tag{2.5c}$$

with

$$\bar{\mu}_n = \frac{n_i q \mu_n}{\alpha}, \ \bar{\mu}_p = \frac{n_i q \mu_p}{\alpha}. \tag{2.5d}$$

In this paper we adhere to the formulation (2.4)-(2.5).

2.1. A particular 1D model problem

We will focus our attention to a particular (hard) 1D model problem which has been supplied by Dr. W.H.A. Schilders, Philips (cf. [10]). Here the problem constants are

$$\epsilon = 1.035918_{10}{}^{-12}, \quad q = 1.6021_{10}{}^{-19}, \ \mu_n = \mu_p = 500, \ n_i = 1.22_{10}{}^{10}, \tag{2.6}$$
$$\alpha = q/kT, \ k = 1.38054_{10}{}^{-23}, \ T = 300.$$

The function R is given by

$$R = \frac{pn - n_i^2}{\tau(p + n + 2n_i)}, \ \tau = 10^{-6}.$$

The doping function D is given by

$$D(x) = 6_{10}{}^{15} + 6_{10}{}^{19}\exp(-(x/7.1_{10}{}^{-5})^2) - 2.15_{10}{}^{18}\exp(-(x/1.15_{10}{}^{-4})^2)$$
$$+ 1.1_{10}{}^{19}\exp(-((x - 8_{10}{}^{-4})/1.3_{10}{}^{-4})^2).$$

The nonlinear operator is defined on the domain $\Omega = [0, 8_{10}{}^{-4}]$. We have three contacts to our semiconductor device (the 1-D model of a transistor): the emitter (E), the basis (B) and the collector (C) (see Figure 1).

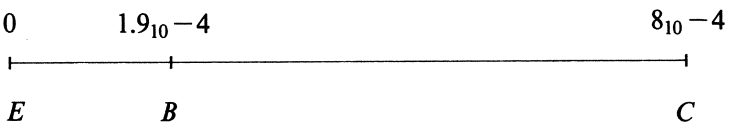

FIGURE 1. The contacts in the 1D transistor problem.

Boundary conditions at the emitter are:

$$p-n+D = 0 \text{ (i.e. vanishing space charge)}, \tag{2.7a}$$

$$\phi_n = V_E, \tag{2.7b}$$

$$J_p = 0. \tag{2.7c}$$

Boundary conditions at the basis:

$$\phi_p = V_B = 0. \tag{2.8}$$

Boundary conditions at the collector:

$$p-n+D = 0, \tag{2.9a}$$

$$\phi_n = V_C, \tag{2.9b}$$

$$\phi_p = V_C. \tag{2.9c}$$

For fifteen different cases, each characterized by a pair of voltages (V_E, V_C), the solution is required.

case	V_E	V_C
0	0.	0.0
1	0.	0.2
2	0.	0.4
3	0.	0.6
4	0.	0.8
5	0.	1.
6	-0.2	1.
7	-0.4	1.
8	-0.6	1.
9	-0.7	1.
10	-0.8	1.
11	-0.85	1.
12	-0.9	1.
13	-0.95	1.
14	-1.	1.

TABLE 2.1. Subsequent voltages at the emitter and collector for which a solution is required.

In figure 2 the doping function $D(x)$ is shown after the transformation $D \rightarrow sign(D)^{10}\log(1+|D|)$.

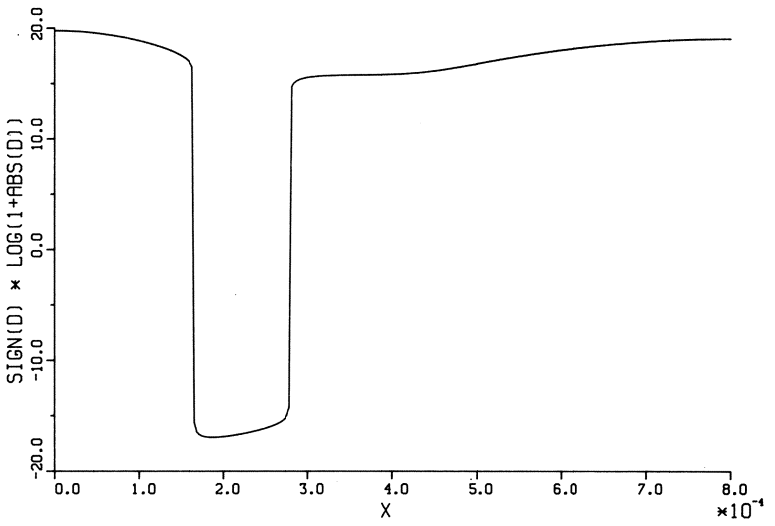

FIGURE 2. The doping profile.

In order to give an impression of the trouble to be expected, we here refer beforehand to the Figures 9-11 in section 7, which show the solutions for the subsequent cases. Especially, we note the moving fronts of ψ,ϕ_n and ϕ_p that arise by slightly decreasing the voltage at the emitter in the range [-0.8, -1]. It is particularly in this range where a difficult part of any numerical solution process is to be encountered.

3. DISCRETIZATION

At the outset of this section we give a short preview of its contents.

In order to abide the law of conservation we use a finite volume technique based on the piecewise constant approximation of J_ψ, J_n and J_p. As a consequence we arrive at a cell-centered version of the well-known Scharfetter-Gummel scheme; this cell-centered version has been introduced by HEMKER (cf. [7]). In the pursuit thereof the discretization of the (internal) boundary condition at the basis will be derived here. We examine how the nonlinear discrete operator depends on the discrete solution.

3.1. Box integration

The interval $\Omega=(x_0, x_N)$ is split up into disjoint *boxes* $B_j=(x_{j-1},x_j), j=1\ (1)\ N$. A point x_j is called a *wall*, a point $x_{j-1/2}=(x_{j-1}+x_j)/2$ is called a *center*. Another set of subintervals $\{D_j\}$ is defined by

$$\begin{aligned} D_0 &= (x_0,x_{1/2}),\\ D_j &= (x_{j-1/2},x_{j+1/2}) \quad j=1\ (1)\ N-1,\\ D_N &= (x_{N-1/2},x_N). \end{aligned}$$

This set is called the set of *dual boxes*. The following conditions should be satisfied:

(i) $x_{j-1}<x_j$,
(ii) $x_0=E, x_N=C$,
(iii) $\exists j^*$ with $0<j^*<N$ such that $x_{j^*}=B$, i.e. the basis B is at the partition-wall between two boxes.

Now, by applying the Gauss divergence theorem in one dimension to the equations (2.4) on the domains B_j we find

$$-J_\psi|_{x_{j-1}}^{x_j} - n_i q \int_{B_j} (e^{\alpha(\phi_p-\psi)} - e^{\alpha(\psi-\phi_n)}) d\Omega = q \int_{B_j} D d\Omega,$$

$$-J_n|_{x_{j-1}}^{x_j} - \frac{n_i q}{\tau}\int_{B_j} \frac{e^{\alpha(\phi_p-\phi_n)}-1}{e^{\alpha(\phi_p-\psi)}+e^{\alpha(\psi-\phi_n)}+2}d\Omega = 0, \tag{3.1}$$

$$-J_p|_{x_{j-1}}^{x_j} + \frac{n_i q}{\tau}\int_{B_j} \frac{e^{\alpha(\phi_p-\phi_n)}-1}{e^{\alpha(\phi_p-\psi)}+e^{\alpha(\psi-\phi_n)}+2}d\Omega = 0, \quad j = 1\,(1)\,N.$$

We can write (3.1) in symbolic form as

$$\mathcal{M}(q) = f \tag{3.2}$$

where q denotes the vector $(\psi,\phi_n,\phi_p)^T$, $\mathcal{M}$ the nonlinear operator in the lefthand side of (3.1) and f the right hand side of (3.1). Further we write

$$\mathcal{M}(q) = \mathcal{N}(q) - r(q) \tag{3.3}$$

where the nonlinear differential operator $\mathcal{N}$ is the part of $\mathcal{M}$ corresponding to the current densities and nonlinear operator r is the part of $\mathcal{M}$ corresponding to the integrals.

3.2. Box discretization

The discretization we use is based on the following approximation of J_ψ, J_n and J_p:

(i) J_ψ,J_n are piecewise constant on the dual set $\{D_j\}$,
(ii) J_p is piecewise constant on the dual set $\{D_j\}$, except for D_{j^*},
(iii) J_p is constant on $D_{L,j^*} \equiv (x_{j^*-1/2},\ B)$ and on $D_{R,j^*} \equiv (B,\ x_{j^*+1/2})$.

Because of (2.5c) and boundary condition (2.8) it should be unnatural to demand that J_p is constant on the whole of D_{j^*}. In fact, also in the continuous case, one can expect that

$$\lim_{x\downarrow B} J_p \neq \lim_{x\uparrow B} J_p. \tag{3.4}$$

That's why an extra degree of freedom for J_p is added by splitting D_{j^*} into D_{L,j^*} and D_{R,j^*}. This extra degree of freedom is annihilated by the boundary condition (2.8). We introduce the notation $J_{\psi,j}$, $J_{n,j}$, $J_{p,j}$ and J_{p,L,j^*}, J_{p,R,j^*}:

$$\begin{aligned} J_\psi &= J_{\psi,j} \text{ on } D_j \\ J_n &= J_{n,j} \text{ on } D_j, \\ J_p &= \begin{cases} J_{p,j} & \text{on } D_j,\ j\neq j^*, \\ J_{p,L,j^*} & \text{on } D_{L,j^*}, \\ J_{p,R,j^*} & \text{on } D_{R,j^*}. \end{cases} \end{aligned} \tag{3.5}$$

Further we introduce the variables $(\psi_j,\phi_{n,j},\phi_{p,j})^T$, $j=1\ (1)\ N$, which are associated with the centers $x_{j-1/2}$ of the boxes B_j. The integrals in the equations (3.1) are approximated by the midpoint quadrature formula

$$n_i q\int_{B_j}(\exp(\alpha(\phi_p-\psi))-\exp(\alpha(\psi-\phi_n)))d\Omega \approx n_i q(\exp(\alpha(\phi_{p,j}-\psi_j))-\exp(\alpha(\psi_j-\phi_{n,j})))\cdot(x_j-x_{j-1}) \equiv S_j,$$

$$q\int_{B_j} D d\Omega \approx qD(x_{j-1/2})\cdot(x_j-x_{j-1}) \equiv F_j, \tag{3.6}$$

$$\frac{n_i q}{\tau}\int_{B_j}\frac{\exp(\alpha(\phi_p-\phi_n))-1}{\exp(\alpha(\phi_p-\psi))+\exp(\alpha(\psi-\phi_n))+2}d\Omega \approx \frac{n_i q}{\tau}\frac{\exp(\alpha(\phi_{p,j}-\phi_{n,j}))-1}{\exp(\alpha(\phi_{p,j}-\psi_j))+\exp(\alpha(\psi_j-\phi_{n,j}))+2}\cdot(x_j-x_{j-1}) \equiv R_j,$$

$$j = 1(1)N.$$

With due regard to (3.4) and applying (3.5), (3.6) the equations (3.1) are approximated by

$$-J_{\psi,j} + J_{\psi,j-1} - S_j = F_j, \quad j = 1(1)N, \tag{3.7a}$$

$$-J_{n,j} + J_{n,j-1} - R_j = 0, \quad j = 1(1)N, \tag{3.7b}$$

$$-J_{p,j} + J_{p,j-1} + R_j = 0, \quad j = 1\,(1)\,j^* - 1,\ j^* + 2\,(1)\,N, \tag{3.7c}$$

and

$$-J_{p,L,j^*} + J_{p,j^*-1} + R_{j^*} = 0, \quad j = j^*, \tag{3.7d}$$

$$-J_{p,j^*+1} + J_{p,R,j^*} + R_{j^*+1} = 0, \quad j = j^* + 1. \tag{3.7e}$$

Now we have to determine also the current densities $J\ldots$ in terms of the variables $(\psi_j, \phi_{n,j}, \phi_{p,j})^T$, $j = 1(1)N$. Because J_ψ is constant on every D_j, we derive

$$J_{\psi,j} = \int_{D_j} \epsilon \nabla\psi d\Omega \Big/ \int_{D_j} 1 d\Omega, \quad j = 0(1)N, \tag{3.8a}$$

by integrating J_ψ over D_j.

Because J_n is constant on every D_j, as well as $\nabla\psi$, we derive from

$$J_n \exp(-\alpha\psi)\nabla(-\alpha\psi) = +\bar{\mu}_n \nabla(\alpha\psi)\exp(-\alpha\phi_n)\nabla(-\alpha\phi_n)$$

by integrating over D_j that

$$J_{n,j} = \bar{\mu}_n \nabla(\alpha\psi) \int_{D_j} \nabla\exp(-\alpha\phi_n) d\Omega \Big/ \int_{D_j} \nabla\exp(-\alpha\psi) d\Omega, \quad j = 0\,(1)\,N. \tag{3.8b}$$

Similarly

$$J_{p,j} = \bar{\mu}_p \nabla(\alpha\psi) \int_{D_j} \nabla\exp(\alpha\phi_p) d\Omega \Big/ \int_{D_j} \nabla\exp(\alpha\psi) d\Omega, \quad j = 0\,(1)\,j^* - 1,\ j^* + 1\,(1)\,N, \tag{3.8c}$$

$$J_{p,L,j^*} = \bar{\mu}_p \nabla(\alpha\psi) \int_{D_{L,j^*}} \nabla\exp(\alpha\phi_p) d\Omega \Big/ \int_{D_{L,j^*}} \nabla\exp(\alpha\psi) d\Omega, \tag{3.8d}$$

$$J_{p,R,j^*} = \bar{\mu}_p \nabla(\alpha\psi) \int_{D_{R,j^*}} \nabla\exp(\alpha\phi_p) d\Omega \Big/ \int_{D_{R,j^*}} \nabla\exp(\alpha\psi) d\Omega. \tag{3.8e}$$

It follows immediately that

$$J_{\psi,j} = \epsilon \frac{\psi_{j+1} - \psi_j}{x_{j+1/2} - x_{j-1/2}}, \quad j = 1\,(1)\,N-1, \tag{3.9a}$$

$$J_{n,j} = \bar{\mu}_n \frac{\exp(-\alpha\phi_{n,j+1}) - \exp(-\alpha\phi_{n,j})}{\exp(-\alpha\psi_{j+1}) - \exp(-\alpha\psi_j)} \cdot \frac{\alpha\psi_{j+1} - \alpha\psi_j}{x_{j+1/2} - x_{j-1/2}}, \quad j = 1(1)N-1, \tag{3.9b}$$

$$J_{p,j} = \bar{\mu}_p \frac{\exp(\alpha\phi_{p,j+1}) - \exp(\alpha\phi_{p,j})}{\exp(\alpha\psi_{j+1}) - \exp(\alpha\psi_j)} \cdot \frac{\alpha\psi_{j+1} - \alpha\psi_j}{x_{j+1/2} - x_{j-1/2}}, \quad j = 1(1)j^* - 1, j^* + 1(1)N. \tag{3.9c}$$

At the basis B:

$$J_{p,L,j^*} = \bar{\mu}_p \frac{\exp(\alpha V_B) - \exp(\alpha\phi_{p,j^*})}{\exp(\alpha\psi_B) - \exp(\alpha\psi_{j^*})} \cdot \frac{\alpha\psi_B - \alpha\psi_{j^*}}{x_{j^*} - x_{j^*-1/2}}, \tag{3.10a}$$

$$J_{p,R,j^*} = \bar{\mu}_p \frac{\exp(\alpha\phi_{p,j^*+1}) - \exp(\alpha V_B)}{\exp(\alpha\psi_{j^*+1}) - \exp(\alpha\psi_B)} \cdot \frac{\alpha\psi_{j^*+1} - \alpha\psi_B}{x_{j^*+1/2} - x_{j^*}}. \tag{3.10b}$$

Because $\nabla\psi$ is constant on D_{j^*} the equality

$$\psi_B = \frac{x_{j^*+1/2} - x_{j^*}}{x_{j^*+1/2} - x_{j^*-1/2}} \psi_{j^*} + \frac{x_{j^*} - x_{j^*-1/2}}{x_{j^*+1/2} - x_{j^*-1/2}} \psi_{j^*+1} \tag{3.11}$$

can be substituted into (3.10).
For expressing the current densities $J_{\psi,0}, J_{n,0}, J_{p,0}$ at the emitter, and the current densities $J_{\psi,N}, J_{n,N}, J_{p,N}$ at the collector, we need to involve the boundary conditions (2.7) and (2.9) respectively.
At the collector:
from (2.9b) and (2.9c) it is easily derived that

$$\psi_C = V_C + \frac{1}{\alpha}\log\left(\frac{D(C)}{2n_i} + \sqrt{\left(\frac{D(C)}{2n_i}\right)^2+1}\right). \tag{3.12}$$

Then, by means of (3.8), we find expressions for $J_{\psi,N}, J_{n,N}, J_{p,N}$ similar to (3.9), except that $x_{j+1/2}$ is replaced by C, ψ_{j+1} by ψ_C, $\phi_{n,j+1}$ and $\phi_{p,j+1}$ by V_C, and j by N.
At the emitter:
the condition (2.7c) implies substituting zero for $J_{p,0}$ in (3.7c). From (2.7a) and (2.7b) it is easily derived that

$$\psi_E = V_E + \frac{1}{\alpha}\log\left(\frac{D(E)}{2n_i} + \sqrt{\left(\frac{D(E)}{2n_i}\right)^2 + \exp(\alpha(\phi_{p,1} - V_E))}\right) \tag{3.13}$$

i.e. an expression in the variable $\phi_{p,1}$.

Then, by means of (3.8), we find expressions for $J_{\psi,0}$, $J_{n,0}$ similar to (3.9a-b), except that $x_{j-1/2}$ is replaced by E, ψ_j by ψ_E, $\phi_{n,j}$ by V_E and j by 0 . Summarizing, we have discretized the equations (2.4), together with the boundary conditions (2.7)-(2.9), into a set of $3N$ nonlinear equations (3.7) with the $3N$ variables ψ_j, $\phi_{n,j}$, $\phi_{p,j}$; $j = 1(1)N$. We can write (3.7) in symbolic form as

$$\mathcal{M}_h(q_h) = f_h \tag{3.14}$$

where $\mathcal{M}_h$ denotes the nonlinear difference operator and f_h the right-hand-side. Further we write

$$\mathcal{M}_h(q_h) = \mathcal{N}_h(q_h) - r_h(q_h) \tag{3.15}$$

where $r_h(q_h)$ is the part of the nonlinear difference operator corresponding to

$$\begin{bmatrix} S_j \\ R_j \\ -R_j \end{bmatrix}, \quad j = 1(1)N,$$

i.e. the discrete source and recombination terms; $\mathcal{N}_h(q_h)$ is the part corresponding to the current densities J. For the solution of nonlinear discrete equations thus obtained we need also derivatives of $\mathcal{N}_h$ and r_h with respect to the discrete variables. For an accurate numerical evaluation of $\mathcal{N}_h(q_h)$ and its derivatives we make use of functions as defined by HEMKER [7] (section 3). Note that at the basis B the derivatives

$$\frac{\partial J_{p,L,j^*}}{\partial \phi_{p,j^*+1}} \quad \text{and} \quad \frac{\partial J_{p,R,j^*}}{\partial \phi^*_{p,j}}$$

are both zero (cf. (3.10)). For an accurate numerical evaluation of the recombination term

$$R(\psi,\phi_n,\phi_p) = \frac{n_i}{\tau}\frac{\exp(\alpha(\phi_p - \phi_n)) - 1}{\exp(\alpha(\phi_p - \psi)) + \exp(\alpha(\psi - \phi_n)) + 2} \tag{3.16}$$

we compute

$$R(\psi,\phi_n,\phi_p) = \frac{n_i}{\tau} f\left(\frac{\alpha(\phi_p - \phi_n)}{2}, \frac{\alpha(\phi_p - 2\psi + \phi_n)}{2}\right) \tag{3.17}$$

where the function f is defined by

$$f(u,v) = \frac{\exp(2u)-1}{\exp(u+v)+\exp(u-v)+2} \tag{3.18}$$

A proper way to evaluate the function f reads:

if $u>\epsilon$ (3.19)

then $-\exp(u-|v|)\cdot\dfrac{\exp(-2u)-1}{1+\exp(-2|v|)+2\exp(-u-|v|)}$

else if $u<-\epsilon$

then $\dfrac{\exp(2u)-1}{\exp(u+v)+\exp(u-v)+2}$

else $\dfrac{TAYLOR(\exp(2u)-1)}{\exp(u+v)+\exp(u-v)+2}$

end if

where ϵ is a small positive number and TAYLOR( ) denotes a Taylor-expansion around $u=0$. The derivatives

$$\frac{\partial R}{\partial \psi}, \quad \frac{\partial R}{\partial \phi_n}, \quad \frac{\partial R}{\partial \phi_p}$$

should be treated likewise, e.g.

$$\frac{\partial R}{\partial \phi_n} = \frac{n_i}{\tau}\cdot -\frac{\alpha}{2}\cdot g\left(\frac{\alpha(\phi_p-\phi_n)}{2}, \frac{\alpha(\phi_p-2\psi+\phi_n)}{2}\right), \tag{3.20a}$$

$$\frac{\partial R}{\partial \phi_p} = \frac{n_i}{\tau}\cdot\frac{\alpha}{2}\cdot g\left(\frac{\alpha(\phi_p-\phi_n)}{2}, \frac{-\alpha(\phi_p-2\psi+\phi_n)}{2}\right) \tag{3.20b}$$

where the function $g(u,v)$ is defined and evaluated by

if $u\geqslant 0$ (3.21)

then $2\exp(|u+v|-2|v|)\cdot\dfrac{1+2\exp(-|u+v|)+\exp(-2|u+v|)}{(1+\exp(-2|v|)+2\exp(-u-|v|))^2}$

else $2\exp(|u+v|+2u)\cdot\dfrac{1+2\exp(-|u+v|)+\exp(-2|u+v|)}{(2+\exp(u-|v|)+\exp(u+|v|))^2}$

end if.

3.3. Properties of the discretized operator

In this subsection we study how the nonlinear discrete operator depends on the discrete solution. We assume the recombination term to be zero and confine ourselves to the dependency on ϕ_p, results for ϕ_n can be derived analogously. We freeze the solution components ψ and ϕ_n and consider the ϕ_p-stencil, at box B_j, defined by the triplet

$$[stp(j,-1),\ stp(j,0),\ \ stp(j,+1)] \tag{3.22a}$$

with

$$stp(j,k) = \frac{\partial(-J_{p,j}+J_{p,j-1})}{\partial \phi_{p,j+k}}, \quad k=-1,0,1. \tag{3.22b}$$

We introduce the notation

$$\Delta_j x \equiv x_{j+1/2}-x_{j-1/2},$$
$$\Delta_j \psi \equiv \psi_{j+1}-\psi_j$$

and the function $s(z):\mathbb{R}\to\mathbb{R}$ by

$$s(z) \equiv \frac{z}{e^z - 1}. \tag{3.23}$$

By straightforward computation it can be verified that the following equalities hold:

$$stp(j,-1) = -\alpha\bar{\mu}_p \exp(\alpha(\phi_{p,j-1}-\psi_j))\frac{s(-\alpha\Delta_{j-1}\psi)}{\Delta_{j-1}x}, \tag{3.24a}$$

$$stp(j,0) = \alpha\bar{\mu}_p \exp(\alpha(\phi_{p,j}-\psi_j))\left\{\frac{s(-\alpha\Delta_{j-1}\psi)}{\Delta_{j-1}x} + \frac{s(\alpha\Delta_j\psi)}{\Delta_j x}\right\}, \tag{3.24b}$$

$$stp(j,+1) = -\alpha\bar{\mu}_p \exp(\alpha(\phi_{p,j+1}-\psi_j))\frac{s(\alpha\Delta_j\psi)}{\Delta_j x}, \tag{3.24c}$$

and

$$stp(j,0) = -(stp(j,-1)+stp(j,+1))+\alpha(-J_{p,j}+J_{p,j-1}). \tag{3.24d}$$

Because $s(z)>0$ for all z, it follows that

$$stp(j,-1)<0,\ stp(j,0)>0,\ stp(j,+1)<0, \tag{3.25}$$

so the ϕ_p-stencils correspond with an $\mathfrak{L}$-matrix. Further, at the exact discrete solution, i.e. when $-J_{p,j}+J_{p,j-1}=0$ is satisfied, it follows from (3.24d) that

$$stp(j,0) = -(stp(j,-1)+stp(j,+1)),$$

so then the $\mathfrak{L}$-matrix possesses also weak diagonal dominance (provided there is at least one stencil corresponding with a Dirichlet boundary condition, cf. [11]).
In the middle of some iterative process to determine the solution, we may well have negative residuals so that the equality (3.24d) implies the loss of diagonal dominance. Therefore ill-conditioning and numerical difficulties can be expected.
We observe from (3.20) and (3.21) that $\frac{\partial(qR)}{\partial\phi_p}>0$ (and $\frac{\partial(-qR)}{\partial\phi_n}>0$). Therefore, if we do not neglect the recombination term, we obtain a ϕ_p-stencil as given by (3.24) except that $stp(j,0)$ has to be enlarged with some positive value $\frac{\partial R_j}{\partial\phi_{p,j}}$.

4. The Newton Method and Expedients

An obvious way of solving the set of nonlinear equations (3.14) is application of the Newton method. Because the Newton method is not globally convergent and the operator $\mathcal{M}_h$ is strongly nonlinear in the variables (ψ,ϕ_n,ϕ_p) we use some additional tools which are considered subsequently in this section:

1) correction transformation,
2) continuation (with boundary voltages as parameter),
3) smoothing of the Newton-iterates.

It turns out that these expedients make the Newton method well applicable. Of course, applying the Newton method directly to (3.14) involves large storage requirements and the solution of large linear systems (it would extremely so in two space dimensions). Therefore it should be applied only for relatively coarse grids. In fact we will use it as a *coarsest grid solver* for multigrid methods which will be treated in Section 5.

4.1. Correction Transformation

The correction transformation, introduced in [8], is a device to transform the Newton-correction $(d\psi, d\phi_n, d\phi_p)$, computed by linearisation with respect to (ψ, ϕ_n, ϕ_p), into the correction for these very variables that would be obtained when linearisation were applied with respect to (ψ, n, p). Because the system in terms of (ψ, n, p) is much less nonlinear, a much better convergence behaviour of the Newton method can be expected. By performing the calculations in terms of (ψ, ϕ_n, ϕ_p) and applying a transformation afterwards, we avoid complications due to the extremely wide range of values of n and p. In this way we take advantage of the benefits of both variable-sets. For an extensive discussion on the correction transformation we refer to [8,7,10].

Let $(\Delta\psi_j, \Delta\phi_{n,j}, \Delta\phi_{p,j})^T, j = 1(1)N$ denote the corrections obtained by applying the Newton method to (3.14) in the variables $(\psi_j, \phi_{n,j}, \phi_{p,j})^T$. The transformation reads:

$$\begin{bmatrix} \Delta\psi_j \\ \Delta\phi_{n,j} \\ \Delta\phi_{p,j} \end{bmatrix} := \begin{bmatrix} \Delta\psi_j \\ \Delta\psi_j \; -\frac{1}{\alpha}\ln(1-\alpha(\Delta\phi_{n,j} \; -\Delta\psi_j)) \\ \Delta\psi_j \; +\frac{1}{\alpha}\ln(1+\alpha(\Delta\phi_{p,j} \; -\Delta\psi_j)) \end{bmatrix} \tag{4.1}$$

When the corrections are small, the transformation does hardly differ from the identity operator.

4.2. Continuation

A further improvement of the global convergence behaviour of the Newton method is obtained by *discrete imbedding*. If we have a solution of (3.14) for $(V_E, V_C)=(a,b)$ and we want a solution for $(V_E, V_C)=(c,d)$, we subsequently solve the problem for

$$(V_E, V_C) = (a.(1-t_j)+t_j c,\ b.(1-t_j)+t_j d),$$

$0=t_0<t_1<t_2<\ldots<t_m=1$. In [10] an efficient stepsize strategy is employed which is here briefly summarized:

(i) We try to solve (3.14) for $t=1$,
(ii) after each iteration, we test on a *divergence criterion A*. If this criterion A is satisfied, we interrupt the process, halve the stepsize and restart; if the criterion is not satisfied, we iterate until a *stopping criterion B* has been satisfied.
(iii) If the stopping criterion has been satisfied, we multiply the stepsize by a factor $\gamma>1$ and try to solve the next subproblem.

In [10] criterion A is determined by a *bandwidth* which provides minimal and maximal values for all iterates and criterion B is determined by a tolerance $TOL(t)$ which is a ℓ_∞-bound for the difference between two successive iterates. (If $t<1$ then $TOL(t) \geqslant TOL(1)$).

4.3. Smoothing

In the subsections 4.1 and 4.2 we pointed out two techniques to improve the global convergence behaviour of the Newton method. Even yet difficulties are encountered when we apply the improved Newton method. As an example consider Fig. 3 which shows subsequent Newton iterates for case $=12$ starting from the solution for case $=11$.

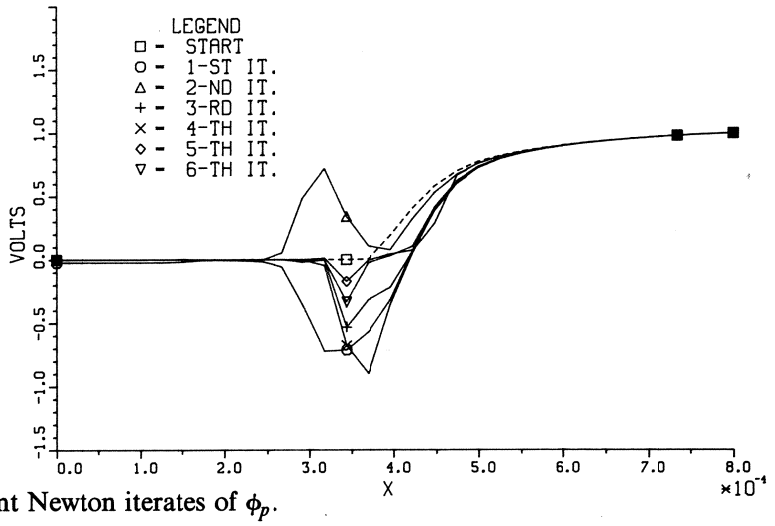

FIGURE 3. Subsequent Newton iterates of ϕ_p.

The dips in the iterates are attended with very small pivot numbers while solving the linear systems. Section 3.3 explains the ill-conditioning whenever there is a large residual somewhere. Artificially increasing the main diagonal of the Jacobian turned out to be not efficient. Simply cutting off the correction at certain points is hardly justifiable because of lack of a more or less general criterion to do so. A more appropriate way of handling the phenomenon sketched above, is to apply relaxation or smoothing sweeps at the beginning of the Newton process (cf. [7]). As a smoother the Collective Symmetric Gauss Seidel relaxation (CSGS) can be used. It is called collective because at each box we solve collectively the three nonlinear equations which arise (employing Newton's method).
We will present here some numerical results to show the effect of smoothing. First we fix a grid by specifying the walls $\{x_j\}$ of the boxes $\{B_j\}$:

$$\begin{aligned} x_j &= E + h_{ER_1}\, j\,, && j = 0,\ldots,3N/16,\\ x_j &= R_1 + h_{R_1B}(j - 3N/16), && j = 3N/16+1,\ldots,N/4,\\ x_j &= B + h_{BR_2}(j - N/4), && j = N/4+1,\ldots,3N/8,\\ x_j &= R_2 + h_{R_2C}(j - 3N/8), && j = 3N/8+1,\ldots,N, \end{aligned} \tag{4.2}$$

where

$$\begin{aligned} h_{ER_1} &= (R_1 - E)/(3N/16),\\ h_{R_1B} &= (B - R_1)/(N/16),\\ h_{BR_2} &= (R_2 - B)/(N/8),\\ h_{R_2C} &= (C - R_2)/(5N/8), \end{aligned}$$

where $D(R_1)=D(R_2)=0$, $R_1<R_2$ and N is a multiple of 16. ($R_1\approx 0.00017$, $R_2\approx 0.00028$; the grid is more or less uniform and satisfies $x_{N/4}=B$; on the coarsest grid possible ($N=16$) the dopefunction D is still fairly well represented).
The set of voltages $\{(V_E, V_C)\}$ for which a solution is required is defined in table 2.1. For each case >0 the solution of the previous case serves as a starting solution; in case 0 we start with $\phi_{n,j}=\phi_{p,j}=0, \forall j$ and ψ is determined by assuming space charge neutrality. We use the correction transformation. For the solution of the linear systems we apply rowscaling followed by rowpivotting. Table 4.1 shows the number of Newton sweeps required to reach a correction with absnorm $<10^{-12}$, and the smallest pivotnumber encountered during the solution process. Table 4.1 also contains the results for the case when in addition a CSGS-sweep is applied each time after a Newton-correction for which the infinity norm of the correction was larger than 0.1.

	No smoothing applied.		Smoothing applied.		
case	Newton-sweeps	Smallest pivot-number	Newton-sweeps	CSGS-sweeps	Smallest pivot-number
0	6	$3_{10}-3$	4	1	$5_{10}-1$
1	5	$2_{10}-4$	5	2	$5_{10}-1$
2	6	$1_{10}-9$	5	2	$5_{10}-1$
3	5	$2_{10}-7$	5	2	$5_{10}-1$
4	5	$1_{10}-7$	5	2	$3_{10}-1$
5	5	$4_{10}-5$	5	2	$3_{10}-1$
6	5	$3_{10}-3$	5	2	$2_{10}-1$
7	5	$3_{10}-3$	5	2	$2_{10}-1$
8	5	$2_{10}-4$	5	2	$2_{10}-1$
9	5	$4_{10}-7$	5	2	$3_{10}-1$
10	6	$1_{10}-7$	6	3	$3_{10}-1$
11	9	$4_{10}-9$	7	3	$2_{10}-1$
12	15	$5_{10}-13$	8	4	$4_{10}-2$
13	13	$2_{10}-11$	7	3	$1_{10}-1$
14	10	$5_{10}-10$	7	3	$1_{10}-1$

TABLE 4.1. Number of Newton- and CSGS-sweeps used, and smallest pivotnumbers; $N=32$.

We observe that in the difficult cases $11-14$ the application of smoothing sweeps has a positive effect on the efficiency and robustness of the Newton method. Experiments for $N=16,64,128$ show results similar to Table 4.1.

5. THE MULTIGRID METHOD

More advanced ways of solving a set of nonlinear equations are the Full Approximation Scheme (FAS), cf. [3] and the Nonlinear Multigrid Method (NMGM), cf. [5]. Both *multigrid methods* are very similar although the NMGM is more general. The multigrid method has already found many specific applications in the fields of elliptic, parabolic and hyperbolic equations and integral equations as well. Recently, also in the field of semiconductor equations research on multigrid methods has been initiated (cf. [1,2,4,7,9]). If well applied, a multigrid method can be optimal in the sense that the rate of convergence is independent of the meshsize. An important advantage of the FAS/NMGM-method is that no large linear systems need to be stored and solved. The subsequent stages of an usual FAS-method, applied to (3.12), are:

1) apply p nonlinear relaxation sweeps; thus we get an approximation q_h of the solution which has a *smooth* residual $d_h \equiv f_h - \mathcal{M}_h(q_h)$,
2) transfer q_h and r_h from Ω_h to a coarser grid Ω_H by means of the respective restriction operators R_H and $\bar{R}_H$,
3) solve (approximately) on Ω_H the equation $\mathcal{M}_H(q_H)=\mathcal{M}_H(R_H q_h)+\bar{R}_H d_h$,
4) interpolate the correction, computed on Ω_H, onto Ω_h and add the correction to q_h,
5) apply q nonlinear relaxation sweeps.

The combination of stage 2,3 and 4 is called the coarse grid correction (CGC). Stage 3 may be obtained by applying a number of σ FAS-cycles on the coarser grid. In this way a recursive procedure is obtained in which a sequence of increasingly coarser grids is used. In this paper we use

$p=q=\sigma=1$ throughout. In the subsections to come we will define precisely the coarse grid correction and the grid transfer operators involved. In Section 6 a significant improvement of the CGC will be introduced. It consists of a solution-dependent adjustment of the restriction of the residual d_h.

5.1. Nested boxes

Let a coarse grid Ω_H, a discretization of Ω, be given by the set of boxes $\{B_{H,j}\}_{j=1(1)N}$. From Ω_H we construct the next finer grid $\Omega_h=\{B_{h,j}\}_{j=1(1)2N}$ by division of each $B_{H,j}$ into two disjoint boxes $B_{h,2j-1}$ and $B_{h,2j}$. By repetition we obtain thus a sequence of increasingly finer grids. By definition all boxes are nested. Of course, the corresponding dual boxes are not nested. For all our numerical experiments in this paper we assume in addition that $B_{h,2j-1}$ and $B_{h,2j}$ have equal size and that the coarsest grid satisfies the definition (4.2).

5.2. Restriction operators

For the problem (3.2) on Ω, let S denote the domain and V the range of nonlinear operator $\mathcal{M}$. For each discretization on Ω_h, we have the spaces S_h and V_h, the discrete analogues of S and V.
Let the restriction operator for right hand side functions

$$\bar{R}_h: V \to V_h \tag{5.1a}$$

be defined by

$$\bar{R}_h f = f_h, \tag{5.1b}$$

$$f_{h,j} = \int_{B_{h,j}} f \, d\Omega, \quad \forall j \text{ at } \Omega_h. \tag{5.1c}$$

It follows for the next coarser grid that

$$(\bar{R}_H f)_j = (\bar{R}_h f)_{2j-1} + (\bar{R}_h f)_{2j}, \quad \forall j \text{ at } \Omega_H. \tag{5.2}$$

By this equality, $\bar{R}_H$ can be defined also on V_h:

$$\bar{R}_H: V_h \to V_H, \tag{5.3a}$$

$$(\bar{R}_H f_h)_j = f_{h,2j-1} + f_{h,2j}, \quad \forall j \text{ at } \Omega_H. \tag{5.3b}$$

The restriction operator for solutions

$$R_h: S \to S_h \tag{5.4a}$$

is defined by

$$R_h s = s_h, \tag{5.4b}$$

$$s_{h,j} = \int_{B_{h,j}} s \, d\Omega / \operatorname{meas}(B_{h,j}), \quad \forall j \text{ at } \Omega_h. \tag{5.4c}$$

If we extend the definition of R_h to the discrete analogues of S, we obtain the well-known fullweighting operator (cf. [3]).

5.3. Prolongation/interpolation

A prolongation transfers a solution from a coarse grid to a finer one:

$$P_h: S_H \to S_h \tag{5.5}$$

A common and simple choice for the prolongation should be linear interpolation. However, two objections against this choice do arise. Firstly, by the use of linear interpolation it is implicitly assumed that the solution behaves like a smooth function on Ω_H. Because of the exponential behaviour of the solution in some areas, this is only true on an unfeasible fine grid. Secondly, linear interpolation does not satisfy here the so called Galerkin condition

$$\bar{R}_H \mathcal{N}_h(P_h s_H) = \mathcal{N}_H(s_H) \tag{5.6}$$

which is a condition that ascertains the reduction of low frequent components in the residual after a CGC (cf. [7]). Hemker has introduced a prolongation which is based on the assumption of smoothness of fluxes, and which satisfies (5.6). Here, we will follow this approach but we choose a different formulation in order to handle also the situation near the inner boundary point B. Fig. 4 depicts how the dual box [L,R] is divided into the boxes [L,M] and [M,R].

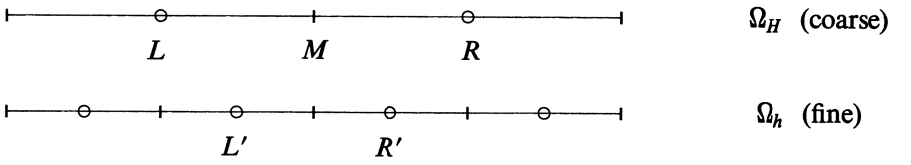

FIGURE 4. Staggering of a coarse and fine grid.

The assumption reads that J_ψ, J_n, J_p are constant on [L,R]. Given the values of the variables (ψ, ϕ_n, ϕ_p) at L and R we wish to compute the values at L' and R'. From (3.8a) it follows that $\psi|_{L'}$ and $\psi|_{R'}$ can be computed by linear interpolation. For ϕ_p we first determine the value at the wall M. Analogously to (3.8c) we derive that

$$\exp(\alpha\phi_p)|_M = \frac{\exp(\alpha\psi)|_M^R}{\exp(\alpha\psi)|_L^R}\exp(\alpha\phi_p)|_L + \frac{\exp(\alpha\psi)|_L^M}{\exp(\alpha\psi)|_L^R}\exp(\alpha\phi_p)|_R \ . \tag{5.7}$$

If we write

$$\Delta\psi = \psi|_R - \psi|_M, \quad \Delta\phi_p = \phi_p|_R - \phi_p|_M \tag{5.8}$$

then

$$\exp(\alpha\phi_p)|_M = \frac{\exp(\alpha\Delta\psi/2)}{\exp(\alpha\Delta\psi/2)+1}\exp(\alpha\phi_p)|_L + \frac{1}{\exp(\alpha\Delta\psi/2)+1}\exp(\alpha\phi_p)|_R \tag{5.9}$$

and we derive the proper numerical evaluation for ϕ_p:

$\phi_p|_M =$

if $\Delta\psi < 0$
then if $\frac{\Delta\psi}{2} - \Delta\phi_p < 0$
then $\phi_p|_R + z(\frac{\Delta\psi}{2}, \frac{\Delta\psi}{2} - \Delta\phi_p)$
else $\phi_p|_L + \frac{\Delta\psi}{2} + z(\frac{\Delta\psi}{2}, -\frac{\Delta\psi}{2} + \Delta\phi_p)$
end if
else if $\frac{\Delta\psi}{2} - \Delta\phi_p < 0$
then $\phi_p|_R - \frac{\Delta\psi}{2} + z(-\frac{\Delta\psi}{2}, \frac{\Delta\psi}{2} - \Delta\phi_p)$
else $\phi_p|_L + z(-\frac{\Delta\psi}{2}, -\frac{\Delta\psi}{2} + \Delta\phi_p)$
end if
end if (5.10)

where the function

$$z: \mathbb{R}^2 \to \mathbb{R} \tag{5.11a}$$

is defined by

$$z(u,v) = \frac{1}{\alpha}\log\left(\frac{\exp(\alpha v)+1}{\exp(\alpha u)+1}\right). \tag{5.11b}$$

Note that

$$|z(u,v)| \leqslant \frac{\log(2)}{\alpha} \text{ for } u \leqslant 0,\ v \leqslant 0. \tag{5.12}$$

By repeating the interpolation procedure, we can compute $\phi_p|_{L'}$ from $\phi_p|_L$ and $\phi_p|_M$, and $\phi_p|_{R'}$ from $\phi_p|_M$ and $\phi_p|_R$. In the particular case that the wall M is the basis B, we do not first determine $\phi_p|_M$ by interpolation, but simply state that

$$\phi_p|_M \equiv \phi_p|_B = V_B \tag{5.13}$$

Analogously, we derive a formula for $\phi_n|_M$:

$\phi_n|_M =$

if $\Delta\psi < 0$
then if $\frac{\Delta\psi}{2} - \Delta\phi_n < 0$

then $\phi_n\|_L$	$-z\left(\frac{\Delta\psi}{2}, \frac{\Delta\psi}{2} - \Delta\phi_n\right)$
else $\phi_n\|_R - \frac{\Delta\psi}{2}$	$-z\left(\frac{\Delta\psi}{2}, -\frac{\Delta\psi}{2} + \Delta\phi_n\right)$

end if
else if $\frac{\Delta\psi}{2} - \Delta\phi_n < 0$

then $\phi_n\|_L + \frac{\Delta\psi}{2}$	$-z\left(-\frac{\Delta\psi}{2}, \frac{\Delta\psi}{2} - \Delta\phi_n\right)$
else $\phi_n\|_R$	$-z\left(-\frac{\Delta\psi}{2}, -\frac{\Delta\psi}{2} + \Delta\phi_n\right)$

end if
end if (5.14)

REMARK 5.1. Because of the equality (5.9) it is obvious that

$$\min\{\phi_p|_L, \phi_p|_R\} \leqslant \phi_p|_M \leqslant \max\{\phi_p|_L, \phi_p|_R\} \tag{5.15}$$

It does *not* follow from (5.9) that $\Delta\psi \ll 0$ always implies $\phi_p|_M \approx \phi_p|_R$ or that $\Delta\psi \gg 0$ always implies $\phi_p|_M \approx \phi_p|_L$, as can be seen by evaluation (5.10).

5.4. Coarse Grid Correction

Let q_n^{old} and q_H^{old} be given approximations to the solution on Ω_h and Ω_H respectively. The CGC is defined by

$$\textit{compute } d_H = \bar{R}_H(f_h - \mathcal{M}_h(q_h^{old})), \tag{5.16a}$$

$$\textit{solve } \mathcal{M}_H(q_H^{new}) = \mathcal{M}_H(q_H^{old}) + d_H, \tag{5.16b}$$

$$\textit{compute } q_h^{new} = q_h^{old} + (P_h q_H^{new} - P_h q_H^{old}), \tag{5.16c}$$

where $\bar{R}_H$ and P_h are the grid transfer operators defined in the previous subsections. Note that q_H^{new} in (5.16b) may be approximated by applying a number of σ FAS-cycles on the grid Ω_H with q_H^{old} as an initial approximation. The approximation q_H^{old} may be given by means of fullweighting:

$$q_H^{old} = R_H q_h^{old}, \tag{5.17a}$$

$$q_{H,j}^{old} = \tfrac{1}{2} q_{h,2j-1}^{old} + \tfrac{1}{2} q_{h,2j}^{old}, \quad \forall j \textit{ at } \Omega_H. \tag{5.17b}$$

Another possibility is to take q_H^{old} equal to q_H^{new} obtained from the last of previous CGCs. The

solution efficiency of many nonlinear problems is not influenced by either choice of q_H^{old}, in our case however it is (see Section 6).

5.5. Full MultiGrid

The Full Multigrid (FMG) algorithm provides the efficient construction of an initial approximation to the solution on a fine grid, once a solution on a coarse grid has been computed (cf. [3,5]). Let Ω_{coarse} be the coarsest grid and Ω_{fine} be the finest one. Intermediate grids are denoted by $l \in \mathbb{N}$. Operators and grid functions do now have l as a subscript instead of h or H. Here we introduce an improvement of the usual FMG in a quasi-Algol description:

procedure BOX-FMG ('$\mathcal{M}_{fine}(q_{fine})=f_{fine}$', *input*:$f_{fine}$, *output*:$q_{fine}$)
begin
(1) **for** l **from** fine -1 **by** -1 **to** coarse
(2) **do** $f_l = \overline{R}_l f_{l+1}$
(3) **end do**
(4) SOLVE ('$\mathcal{M}_{coarse}(q_{coarse})=f_{coarse}$', *input*:$f_{coarse}$, *output*:$q_{coarse}$)
(5) **for** l **from** coarse $+1$ **to** fine
(6) **do** $q_l = P_l q_{l-1}$
(7) **to** γ
(8) **do** FAS ('$\mathcal{M}_l(q_l)=f_l$', *input*:f_l, *in/output*:q_l)
(9) **end do**
(10) **end do**
end procedure (5.18)

where $\overline{R}_l$ is defined by (5.3). The improvement is in the lines (1)-(3) of the procedure. The gridfunction f_l is independent of q_l, the components represent

$$f_{l,j} = \int_{B_j} D \, d\Omega \tag{5.19}$$

i.e. the dopefunction integrated over box B_j. By means of (1)-(3) we compute the integral as a Riemann-sum over a larger number of subintervals. This is more accurate because D is a rapidly varying function. In the numerical experiments to come we use $\gamma=1$ throughout. For SOLVE( ) we use the techniques of Section 4.

6. Adaptation of the Coarse Grid Correction

Hemker successfully applied boxcentered multigrid FAS iteration to the forward and the reverse biased diode problem (cf. [7]). A key-feature in his application is the prolongation based on locally constant fluxes. This prolongation has been reformulated and made suitable for the transistorproblem in Section 5. Application of the same MG-algorithm to the transistorproblem, gives rise to a complication in the CGC due to drastically varying problem coefficients. This complication and possible remedies are the topics of this section.

6.1. Improper solution transfer

The first attempt of applying multigrid to our specific problem was done by employing BOX-FMG with only two grids. The coarse grid problem (5.16b), within the CGC of FAS, was to be solved up to machine-accuracy by means of Newton combined with smoothing (to which we shall henceforth refer to by the abbreviation Newton-CSGS). For several cases of our testproblem it turned out that the twogrid-algorithm gets stuck precisely at stage (5.16b) of the CGC. This is remarkable because Newton-CSGS was shown in section 4.3 to be successful for $\mathcal{M}_H(q_H)=f_H$ even for rather coarse grids. Apparently f_H is within an appropriate range of $\mathcal{M}_H$ while the right handside of (5.16b) may be outside such a proper range of $\mathcal{M}_H$. The computational difficulty occurs in CSGS on the coarse grid exactly where one or more of the three solution components depicts a steep gradient and indeed that is causing the trouble. Consider two adjacent boxes B_L^h and B_R^h on the fine grid which together

constitute a box B^H on the coarse grid. Because of the steep gradient it may well occur that the problem coefficients, i.e. the entries of the Jacobian of $\mathcal{M}_h$, show a quite different order of magnitude on B_L^h and B_R^h respectively. Gridfunction d_H, the restriction of the residual, is dominated by the fine grid box with the large coefficients. On the other hand the operator $\mathcal{M}_H$ is generated by the particular choice of q_H^{old}. This particular choice may be full weighting applied to q_h^{old}, or the last q_H available, etc. It is important to note that because of the steep gradient in q_h^{old} there is a large range of possible values for q_H^{old} at B^H. Depending on the choice of q_H^{old} the operator $\mathcal{M}_H$ may have either large or small coefficients at box B^H due to the exponential behaviour of the entries in the Jacobian as a function of the solution. In the case of small coefficients, the righthandside of (5.16b) may become out of the appropriate range for $\mathcal{M}_H$ (d_H does not depend on the particular choice of q_H^{old}) and the two grid-algorithm gets stuck.

REMARK 6.1. Even in the case where (5.16b) is numerically solvable, trouble will occur for the same reason. Suppose that in (5.16) q_h^{old} solves the discrete problem; then mathematically, $d_H=0$ and therefore $q_h^{new}=q_h^{old}$. However, we have a finite machine accuracy δ and the entries on the main diagonal corresponding with B_L^h and B_R^h may differ in orders of magnitude. e.g. 10^{-5} versus 10^4. The entry on the main diagonal of the Jacobian on the coarse grid at B^H may be about 1. The result of the CGC will be that the solution on the fine grid will be distorted by approximately $10^4\delta$.

We will now confirm the foregoing by considering our discretized problem in more detail. Consider the center of the ϕ_p-stencil given by (3.24b) and let us suppose that ψ is monotonous on $[x_{j-3/2},x_{j-1/2}]$; then either $s(-\alpha\Delta_{j-1}\psi)\geqslant 1$ or $s(\alpha\Delta_j\psi)\geqslant 1$. If both $|\Delta_{j-1}\psi|$ and $|\Delta_j\psi|$ are sufficiently small then $stp(j,0)$ is approximated by

$$stp(j,0)\approx\alpha\bar{\mu}_p\exp(\alpha(\phi_{p,j}-\psi_j))\cdot\left(\frac{1}{\Delta_{j-1}x}+\frac{1}{\Delta_j x}\right).$$

If both $|\Delta_{j-1}\psi|$ and $|\Delta_j\psi|$ are sufficiently large then $stp(j,0)$ is approximated by

$$stp(j,0)\approx\alpha\bar{\mu}_p\exp(\alpha(\phi_{p,j}-\psi_j))\cdot\begin{cases}\alpha\dfrac{\Delta_{j-1}\psi}{\Delta_{j-1}x} & \text{if } \Delta_{j-1}\psi\geqslant 0,\\ -\alpha\dfrac{\Delta_j\psi}{\Delta_j x} & \text{if } \Delta_j\psi\leqslant 0\end{cases}$$

These approximations show that indeed the ϕ_p-stencil is extremely sensitive to the difference $(\phi_{p,j}-\psi_j)$. Hence the ϕ_p-stencil on the coarse grid is sensitive to how $\phi_{p,j}$ and ψ_j on the coarse grid are determined from their counterparts on the fine grid. If q_H^{old} is determined by applying full weighting (linear interpolation) to q_h^{old} then

$$stp(j/2,0)\approx\exp\left(-\frac{\alpha}{2}|\Delta_j(\phi_p-\psi)|\right)\cdot\max\{stp(j-1,0),\ stp(j,0)\}$$

where $stp(j-1,0)$, $stp(j,0)$ (j even) are defined at the fine grid Ω_h and $stp(j/2)$ at the coarse grid Ω_H. If $(\phi_p-\psi)$ shows a steep gradient then indeed

$$stp(j/2)\ll\max\{stp(j-1,0),\ stp(j,0)\}.$$

NOTE. The possible occurrance of the above sketched phenomenon has already been notified (for general nonlinear problems) by A. BRANDT (cf. [3], p. 279), where he discusses how the transferred solution (i.e. q_H^{old}) implicitly determines the problem coefficients on the coarse grid.

6.2. Possible remedies

Let L and R be the centers of the two adjacent boxes B_L^h and B_R^h on the fine grid Ω_h which together constitute a coarse grid box B_M^H with center M on the coarse grid Ω_H (see figure 5).

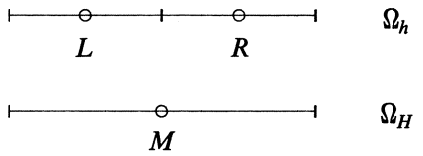

FIGURE 5. Nested boxes.

Let us assume that $\frac{\partial \psi}{\partial x} = c$ is constant on $B_L^h \cup B_R^h$. The centers of the ϕ_p-stencils at L,R are then determined by the coefficients $a_L^h \equiv \exp(\alpha(\phi_p - \psi)|_L)\bar{c}$, $a_R^h \equiv \exp(\alpha(\phi_p - \psi)|_R)\bar{c}$ respectively and the center of the ϕ_p-stencil at M by $a_M^H \equiv \exp(\alpha(\phi_p - \psi)|_M)\bar{c}$ with $\bar{c} = \alpha^2 \bar{\mu}_p |c|$ (see section 6.1). Let $\Delta_M(\phi_p - \psi)$ denote the variation $\Delta_M(\phi_p - \psi) = (\phi_p - \psi)|_R - (\phi_p - \psi)|_L$. The solution at M on the coarse grid somehow relates to the solution at L and R on the fine grid (for instance by means of the full weighting restriction). If $\Delta_M(\phi_p - \psi)$ is small (a smooth solution) then obviously a_M^H does not differ much from either a_L^h or a_R^h. If $\Delta_M(\phi_p - \psi)$ is large (a steep gradient in the solution) then a_M^H may differ orders of magnitude from both a_L^h and a_R^h, and therefore the MG-algorithm may get stuck as was pointed out in the previous subsection. A radical remedy to meet this situation is to prevent $\Delta_M(\phi_p - \psi)$ from getting large, i.e. to introduce local refinement of the mesh just where the solution has a large variation $\Delta_M(\phi_p - \psi)$, e.g. by means of equidistributing the variation. However, we want to be able to find solutions without much refinement, in order to apply coarse grids in our MG-algorithm. Besides, a solution without much resolution can serve as a guide for where a local mesh refinement should take place. For this reasons we resort to another remedy. Let us consider the CGC (5.16). Let $d_h(L), d_h(R)$ be the residuals at L, R (e.g. for the third equation (3.7c) only). At M the difference between q_H^{new} and q_H^{old} may have the order of magnitude $d_H(M)/a_M^H$ with $d_H(M) = d_h(L) + d_h(R)$. Because of (5.16c) at either L, R, or both L and R a correction with order of magnitude $d_H(M)/a_M^H$ is added to the solution q_h^{old}. Assume that (because of a steep gradient in the solution) the inequality

$$(min\{a_L^h, a_R^h\} <) a_M^H \ll \max\{a_L^h, a_R^h\}$$

holds. Therefore

$$d_H(M)/a_M^H \gg (d_h(L) + d_h(R))/\max\{a_L^h, a_R^h\} ,$$

which implies that the correction that will be transferred to the fine grid becomes far too large and the solution q_h^{old} gets spoiled. A way to prevent this situation is to multiply the restricted residual d_H with

$$\theta_M^H \equiv \frac{a_M^H}{\max\{a_L^h, a_R^h\}}, \quad 0 < \theta_M^H \leq 1, \tag{6.1}$$

at each center M. For a smooth part of the solution this fraction will be near to 1, for a rapidly varying part of the solution it will be near to 0 so that the solution q_h^{old} will be preserved. The foregoing is the motivation for the following modification of the FAS-algorithm (MFAS) using the notation of section 5.5:

Procedure MFAS ('$\mathcal{M}_l(q_l)=f_l$', *input* :f_l, *in/output*:q_l)
begin
(1) **if** l=coarse
(2) **then** SOLVE ('$\mathcal{M}_{coarse}(q_{coarse})=f_{coarse}$', *input*:$f_{coarse}$, *in/output*:$q_{coarse}$)
(3) **else** RELAX('$\mathcal{M}_l(q_l)=f_l$', *input*:f_l, *in/output*:q_l)
(4) $d_{l-1}:=\bar{R}_{l-1}(f_l-\mathcal{M}_l(q_l))$
(5) $q_{l-1}:=R_{l-1}q_l$ (optional !)
(6) $d_{l-1}:=\Theta_{l-1}(q_{l-1}, q_l)d_{l-1}$
(7) $d_{l-1}:=d_{l-1}+\mathcal{M}_{l-1}(q_{l-1})$ (6.2)
(8) $s_{l-1}:=q_{l-1}$
(9) **to** σ
(10) **do** MFAS ('$\mathcal{M}_{l-1}(q_{l-1})=d_{l-1}$', *input*:$d_{l-1}$,*in/output*:q_{l-1})
(11) **end do**
(12) $q_l:=q_l + P_l q_{l-1}-P_l s_{l-1}$
(13) RELAX('$\mathcal{M}_l(q_l)=f_l$', *input*:f_l, *in/output*:q_l)
(14) **end if**
end procedure

Here Θ_{l-1} represents a diagonal matrix $\mathbb{R}^{3N(\Omega_{l-1})}\to\mathbb{R}^{3N(\Omega_{l-1})}$ ($N(\Omega_{l-1})$ denotes the number of boxes at Ω_{l-1}). It is defined by

$$\Theta_{l-1}d_{l-1} = (\theta_{l-1,1}d_{l-1,1},...,\theta_{l-1,j}d_{l-1,j},...,\theta_{l-1,N(\Omega_{l-1})}d_{l-1,N(\Omega_{l-1})})^T$$

with $d_{l-1,j}\in\mathbb{R}^3$, $\theta_{l-1,j}:\mathbb{R}^3\to\mathbb{R}^3$ and

$$\theta_{l-1,j} \equiv \begin{bmatrix} \theta_{l-1,j,1} & 0 & 0 \\ 0 & \theta_{l-1,j,2} & 0 \\ 0 & 0 & \theta_{l-1,j,3} \end{bmatrix}$$

($\theta_{l-1,j,k}\in\mathbb{R}$, $k = 1, 2, 3$).

We will consider two specific choices for the $\theta_{l-1,j,k}$; either choice has the form:

$$\theta_{l-1,j,1} = 1, \tag{6.3a1}$$

$$\theta_{l-1,j,2} = \min\{2\eta_{l-1,j}, 1\},\ \eta_{l-1,j}\in\mathbb{R}, \tag{6.3a2}$$

$$\theta_{l-1,j,3} = \min\{2\xi_{l-1,j}, 1\},\ \xi_{l-1,j}\in\mathbb{R}. \tag{6.3a3}$$

CHOICE 1:

$$\begin{aligned} \eta_{l-1,j} &\equiv \exp(\alpha(\psi_j^{l-1}-\phi_{n,j}^{l-1}))/\max_{i=0,-1}\exp(\alpha(\psi_{2j+i}^{l}-\phi_{n,2j+i}^{l})), \\ \xi_{l-1,j} &\equiv \exp(\alpha(\phi_{p,j}^{l-1}-\psi_j^{l-1}))/\max_{i=0,-1}\exp(\alpha(\phi_{p,2j+i}-\psi_{2j+i}^{l})). \end{aligned} \tag{6.3b}$$

The superscripts $l-1, l$ refer to Ω_{l-1}, Ω_l respectively.

CHOICE 2:

$$\begin{aligned} \eta_{l-1,j} &\equiv \exp(-|\alpha(\psi_{2j}^{l}-\phi_{n,2j}^{l})-\alpha(\psi_{2j-1}^{l}-\phi_{n,2j-1}^{l})|), \\ \xi_{l-1,j} &\equiv \exp(-|\alpha(\phi_{p,2j}^{l}-\psi_{2j}^{l})-\alpha(\phi_{p,2j-1}^{l}-\psi_{2j-1}^{l})|). \end{aligned} \tag{6.3c}$$

The first component of the restricted residual needs not to be adjusted. Choice 1 originates from the evaluation of (6.1); choice 2 depends on the fine grid solution q_l only. By means of (6.3a2-a3) the numbers $\theta_{l-1,j,2}$ and $\theta_{l-1,j3}$ are rounded off upwards to 1 when $\eta_{l-1,j}, \xi_{l-1,j}$ are $\geqslant 1/2$.

Summarizing, we observe the following from (6.2)-(6.3):
i) where q_l is smooth, d_{l-1} will not be suppressed;
ii) where q_l depicts a steep gradient, d_{l-1} may be strongly suppressed;
iii) let Ω_0 be some fixed grid, then, for $l \to \infty$, the matrix Θ_{l-1} becomes asymptotically the identity matrix;
iv) by a proper local mesh refinement the suppression of d_{l-1} will decrease.

The performance of the modified FAS-algorithm will be shown and discussed in section 7.

In the nonlinear multigrid algorithm as proposed by HACKBUSCH (cf. [5], section 9), the restricted residual d_{l-1} is divided by a global parameter $s \geqslant 1$ and the resulting coarse grid correction is multiplied by s. The division by an appropriate s ensures that the righthandside of the coarse grid equation is within an appropriate range of the coarse grid operator $\mathcal{M}_{l-1}$. There are two main differences with our approach. Firstly the same number s is used at each different box. Secondly, within our class of problems we have to omit the multiplification of the correction by s. By the same reasoning as in the beginning of this section it can be seen that such a multiplification would result in a far too large correction and thereby a dip or peak in the fine grid solution. In recent work of HACKBUSCH and REUSKEN (cf. [6]) a global parameter ψ is proposed by which the coarse grid correction should be damped. For a limited class of problems an appropriate ψ can be computed. Important differences with our approach are the following:
i) ψ is a damping parameter for the correction, in stead of the residual;
ii) ψ is a global parameter, i.e. the same ψ is used at each different box;
iii) after sufficient FAS-sweeps the damping parameter ψ converges to 1, the parameters $\theta_{l-1,j,2}$, $\theta_{l-1,j,3}$ do not and should not necessarily converge to 1, as can be seen from remark 6.1;
iv) the ψ-parameter is meant to enlarge the domain of guaranteed convergence on the analogy of the damping parameter in the Newton method, the Θ_{l-1}-operator is meant to deal with discrepancies between the operators $\mathcal{M}_{l-1}$ and $\mathcal{M}_l$ due to rapidly varying problem coefficients.

The idea of suppressing the restricted residual at grid points where a coarse grid correction is apparently harmful, and thereby preserving the last obtained fine grid solution, may cover a wider field of applications within the multigrid philosophy.

REMARK 6.2. One may consider the possibility of using the nonlinear interpolation as mentioned in section 5.3 for the construction of a restriction operator for the solution. Then $\psi|_M$ is defined by linear interpolation between $\psi|_L$ and $\psi|_R$, and $\phi_p|_M$, $\phi_n|_M$ are defined by (5.10), (5.14) respectively (see also figure 5). It can be derived from (5.9) that

$$\exp(\alpha(\phi_p - \psi)|_M) = \frac{1}{\exp(\alpha\Delta\psi/2)+1} \exp(\alpha(\phi_p - \psi)|_L) + \frac{\exp(\alpha\Delta\psi/2)}{\exp(\alpha\Delta\psi/2)+1} \exp(\alpha(\phi_p - \psi)|_R).$$

Hereby it is easily seen that again it may occur that $0 < a_M^H / \max_{L,R}\{a_L^h, a_R^h\} \ll 1$ (see section 6.1), and therefore, also for this solution transfer, the Θ-function within MFAS cannot be dispensed with. Furthermore, the underlying assumption of this solution transfer is that J_ψ, J_n, J_p are piecewise constant on the fine dual grid, which is not consistent with J_ψ, J_n, J_p being piecewise constant on the coarse dual grid. Indeed this particular solution transfer leads to poor performance of the MFAS-procedure (see section 7).

7. NUMERICAL RESULTS

In this section we investigate the performance of our nonlinear multigridalgorithm. We focus our attention on the effects of local suppressing of the restricted residual and the choice of the coarse grid solution. The residual norm ($\|\cdot\|_{res}$) that we use is the maximum norm of the scaled residual, at level l the said scaling is done by multiplying the residual at each box with the inverse of the 3×3-matrix

$$\left[\frac{\partial \mathcal{M}_l|_{x_{j-1/2}}}{\partial(\psi_j^l,\ \phi_{n,j}^l,\ \phi_{p,j}^l)^T} \right].$$

The performance of the MFAS-algorithm is shown in the tables 7.1-7.3. Those three tables cover three possibilities for line (5) in (6.2):

- table 7.1 corresponds to omitting line (5) in (6.2), i.e. q_{l-1} is determined by taking the last available solution on Ω_{l-1};
- table 7.2 corresponds to taking the full weighting (linear interpolation) operator for R_{l-1};
- table 7.3 finally, shows the performance when we use the nonlinear interpolation of section 5.3 for the restriction operator R_{l-1} (see also remark 6.2).

In the headings of the tables we use the following abbreviations:

after FMG : the column shows the scaled norm of the residual, after application of BOX-FMG (see (5.18), $\gamma=1$). In each case >0 we obtain a starting approximation of the solution on the coarsest grid by means of continuation and application of Newton-CSGS (see section 4.3).

MFAS, 10^{-1}red. : the average number of MFAS-sweeps necessary to obtain an additional reduction factor 10^{-1} of the residualnorm after the application of BOX-FMG;

no Θ_{l-1} : no local suppression of d_{l-1} is applied;

$\Theta_{l-1} \equiv$ Choice 1 : Θ_{l-1} corresponds to (6.3b);

$\Theta_{l-1} \equiv$ Choice 2 : Θ_{l-1} corresponds to (6.3c);

case : see table 2.1.

For the tables 7.1-7.3 the multigrid procedures are applied with 3 grids, defined by (4.2) with $N = 16, 32, 64$ respectively. In the event of no convergence the symbol $\star$ is written.

	no Θ_{l-1}		$\Theta_{l-1} \equiv$ Choice 1		$\Theta_{l-1} \equiv$ Choice 2	
case	after FMG	#MFAS, 10^{-1} red.	after FMG	#MFAS, 10^{-1} red.	after FMG	#MFAS, 10^{-1} red.
0	$4.1_{10}-4$	0.66	$4.1_{10}-4$	0.66	$4.1_{10}-4$	0.66
1	$8.8_{10}-4$	0.88	$8.8_{10}-4$	0.73	$8.9_{10}-4$	0.78
2	$\star$		$1.2_{10}-3$	0.85	$1.2_{10}-3$	0.85
3	$\star$		$1.2_{10}-3$	1.03	$1.2_{10}-3$	1.03
4	$\star$		$7.1_{10}-4$	1.06	$7.1_{10}-4$	1.06
5	$\star$		$5.7_{10}-4$	0.89	$5.7_{10}-4$	0.89
6	$\star$		$5.7_{10}-4$	0.89	$5.7_{10}-4$	0.89
7	$\star$		$5.7_{10}-4$	0.89	$5.7_{10}-4$	0.89
8	$5.6_{10}-4$	0.89	$5.6_{10}-4$	0.89	$5.6_{10}-4$	0.89
9	$6.6_{10}-4$	0.87	$5.7_{10}-4$	0.90	$5.2_{10}-4$	0.91
10	$1.3_{10}-3$	0.88	$1.1_{10}-3$	0.82	$2.0_{10}-3$	1.09
11	$1.3_{10}-3$	1.25	$1.3_{10}-3$	1.25	$1.3_{10}-3$	1.46
12	$9.1_{10}-4$	2.01	$9.1_{10}-4$	2.01	$8.9_{10}-4$	2.23
13	$1.9_{10}-3$	2.19	$1.9_{10}-3$	2.19	$1.8_{10}-3$	2.78
14	$2.5_{10}-3$	1.76	$2.5_{10}-3$	1.77	$5.6_{10}-3$	1.75

TABLE 7.1. Performance of MFAS; coarse grid solutions defined by taking the last available ones; 3 grids: $N = 16, 32, 64$ respectively.

	no Θ_{l-1}		$\Theta_{l-1} \equiv$ Choice 1		$\Theta_{l-1} \equiv$ Choice 2	
case	after FMG	#MFAS, 10^{-1} red.	after FMG	#MFAS, 10^{-1} red.	after FMG	#MFAS, 10^{-1} red.
0	$4.5_{10}-4$	0.80	$4.5_{10}-4$	0.80	$4.5_{10}-4$	0.80
1	$9.8_{10}-4$	1.07	$9.8_{10}-4$	1.07	$1.1_{10}-3$	0.98
2	*		$7.5_{10}-4$	1.15	$8.6_{10}-4$	1.14
3	*		*		*	
4	*		*		*	
5	*		*		*	
6	*		*		*	
7	*		$6.5_{10}-4$	1.38	$6.5_{10}-4$	1.38
8	$6.4_{10}-4$	1.40	$6.4_{10}-4$	1.37	$6.4_{10}-4$	1.37
9	$7.1_{10}-4$	1.54	$6.6_{10}-4$	1.37	$5.1_{10}-4$	1.25
10	$1.2_{10}-3$	2.59	$1.2_{10}-3$	2.52	$2.4_{10}-3$	1.58
11	$7.6_{10}-4$	1.22	$7.6_{10}-4$	1.22	$8.9_{10}-4$	1.42
12	$1.3_{10}-3$	1.75	$1.3_{10}-3$	1.74	$1.2_{10}-3$	1.75
13	$5.7_{10}-3$	4.66	$5.7_{10}-3$	4.66	$6.1_{10}-3$	4.15
14	$2.8_{10}-3$	2.44	$2.6_{10}-3$	2.43	$5.2_{10}-3$	1.62

TABLE 7.2. Performance of MFAS; coarse grid solutions defined by applying fullweighting to the fine grid solutions; 3 grids: $N = 16, 32, 64$ respectively.

	no Θ_{l-1}		$\Theta_{l-1} \equiv$ Choice 1		$\Theta_{l-1} \equiv$ Choice 2	
case	after FMG	#MFAS, 10^{-1} red.	after FMG	#MFAS, 10^{-1} red.	after FMG	#MFAS, 10^{-1} red.
0	$4.5_{10}-4$	0.80	$4.5_{10}-4$	0.80	$4.5_{10}-4$	0.80
1	$1.0_{10}-3$	1.09	$1.0_{10}-3$	0.98	$1.1_{10}-3$	1.05
2	*		*		*	
3	*		*		*	
4	*		*		*	
5	*		*		*	
6	*		*		*	
7	*		*		*	
8	*		*		*	
9	*		*		*	
10	$1.2_{10}-3$	3.85	$1.4_{10}-3$	4.06	$2.2_{10}-3$	1.78
11	$8.0_{10}-4$	1.53	$7.9_{10}-4$	1.53	$9.9_{10}-4$	1.43
12	$1.8_{10}-3$	2.00	$1.7_{10}-3$	1.97	$1.7_{10}-3$	1.99
13	$7.7_{10}-3$	5.35	$7.5_{10}-3$	5.23	$8.0_{10}-3$	4.19
14	$2.3_{10}-3$	4.28	$2.7_{10}-3$	4.02	$6.2_{10}-3$	1.58

TABLE 7.3. Performance of MFAS; coarse grid solutions defined by applying a restriction based on constant fluxes to the fine grid solutions; 3 grids: $N = 16, 32, 64$ respectively.

The poor results of table 7.3 were to be expected after remark 6.2. Table 7.2 shows that the use of a Θ-operator is not sufficient on his own to guarantee convergence, apparently the full weighting approximation of the fine grid solution on the coarse grid may be a poor one (case 3-6). Table 7.1 shows that the use of a Θ-operator combined with a proper choice of the coarse grid solution is essential for the sake of robustness of the MFAS-procedure, especially Choice 1 for the Θ-operator is favorable because then we have convergence for all cases and it does not slow down convergence in the cases where a Θ-operator turns out to be superfluous. Further we observe that mere application of BOX-FMG, without further MFAS-sweeps, already gives fairly accurate results which may be well enough for practical purposes. If desired, one could use BOX-FMG as a cheap provider of a starting approximation for the Newton-method, results thereof are shown in table 7.4 (the algorithm parameters used are the ones of table 7.1, with Choice 1). However, in the case of more space dimensions this hybrid combination is probably inferior to BOX-FMG extended with further MFAS-sweeps, considered from the viewpoint of complexity and storage requirements.

case	after FMG	Newton-sweeps	Smallest pivot-number
0	$4.1_{10}-4$	4	$5_{10}-1$
1	$8.8_{10}-4$	4	$5_{10}-1$
2	$1.2_{10}-3$	4	$5_{10}-1$
3	$1.2_{10}-3$	4	$5_{10}-1$
4	$7.1_{10}-4$	4	$5_{10}-1$
5	$5.7_{10}-4$	4	$5_{10}-1$
6	$5.7_{10}-4$	4	$5_{10}-1$
7	$5.7_{10}-4$	4	$5_{10}-1$
8	$5.6_{10}-4$	4	$5_{10}-1$
9	$5.7_{10}-4$	4	$5_{10}-1$
10	$1.1_{10}-3$	4	$5_{10}-1$
11	$1.3_{10}-3$	5	$3_{10}-1$
12	$9.1_{10}-4$	5	$3_{10}-1$
13	$1.9_{10}-3$	5	$2_{10}-1$
14	$2.5_{10}-3$	5	$1_{10}-1$

TABLE 7.4. Performance of BOX-FMG followed by Newton; in the first column the scaled norm of the residual after BOX-FMG, in the second colum, the number of Newton sweeps required to reach a correction with absnorm $<1_{10}-12$, in the third column the smallest pivotnumber encountered during the Newton-process on the finest grid.

Comparison of table 7.4 with table 4.1 shows that in the cases 11-14 there is a substantial reduction of Newton-sweeps.

In order to investigate how the convergence rate of the MFAS-algorithm depends on the meshsize we repeat the experiments of table 7.1, but now for 4 grids with $N = 16, 32, 64, 128$ respectively; the results are shown in table 7.5.

	no Θ_{l-1}		$\Theta_{l-1} \equiv$ Choice 1		$\Theta_{l-1} \equiv$ Choice 2	
case	after FMG	#MFAS, 10^{-1} red.	after FMG	#MFAS, 10^{-1} red.	after FMG	#MFAS, 10^{-1} red.
0	$6.5_{10}-4$	0.84	$6.5_{10}-4$	0.84	$6.5_{10}-4$	0.84
1	$6.5_{10}-4$	0.84	$6.5_{10}-4$	0.84	$6.5_{10}-4$	0.84
2	*		$6.5_{10}-4$	0.84	$6.5_{10}-4$	0.84
3	*		$6.5_{10}-4$	0.84	$6.5_{10}-4$	0.84
4	*		$6.5_{10}-4$	0.89	$6.5_{10}-4$	0.89
5	*		$6.5_{10}-4$	0.88	$6.5_{10}-4$	0.88
6	*		$5.9_{10}-4$	0.89	$5.9_{10}-4$	0.89
7	*		$2.4_{10}-4$	0.94	$2.4_{10}-4$	0.94
8	$2.4_{10}-4$	0.94	$2.4_{10}-4$	0.94	$2.4_{10}-4$	0.94
9	$2.4_{10}-4$	0.91	$2.4_{10}-4$	0.91	$2.5_{10}-4$	0.91
10	$2.1_{10}-4$	0.84	$1.8_{10}-4$	0.85	$9.9_{10}-5$	0.95
11	$1.6_{10}-4$	1.53	$1.6_{10}-4$	1.53	$1.7_{10}-4$	1.71
12	$1.6_{10}-4$	2.24	$1.6_{10}-4$	2.24	$1.7_{10}-4$	2.53
13	$4.5_{10}-4$	2.10	$4.5_{10}-4$	2.10	$4.8_{10}-4$	2.48
14	$1.2_{10}-3$	1.85	$1.3_{10}-3$	1.85	$1.7_{10}-3$	1.47

TABLE 7.5. Performance of MFAS; coarse grid solutions defined by taking the last available ones; 4 grids: $N = 16, 32, 64, 128$ respectively.

For some cases we observe that the work required for an extra digit slightly increases, for other cases it decreases.

For two typical cases, case $= 4$ and case $= 12$, we investigate the grid-dependence of the multigrid convergence in detail. In figure 6 we show the 10-logarithm of the scaled residual norms after subsequent FAS-sweeps, starting from the result obtained by BOX-FMG. The coarsest grid contains 16 boxes, for the finest grid we take 32, 64, 128 and 256 boxes respectively; Θ is defined by Choice 1. We observe that the multigrid convergence becomes grid-independent when the meshsize of the finest grid decreases.

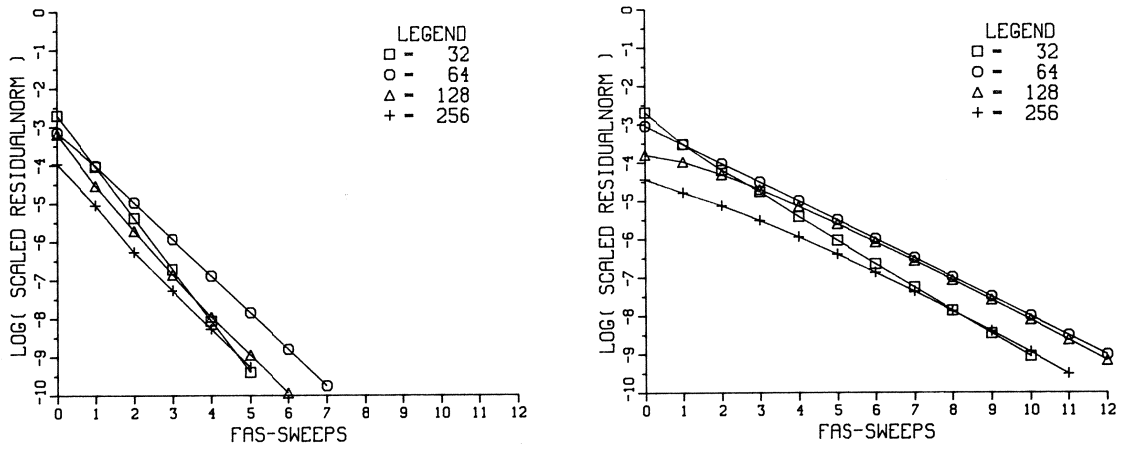

a. case = 4. b. case = 12.

FIGURE 6. Multigrid convergence histories; the coarsest grid numbers 16 boxes.

In order to give some insight into the behaviour of the Θ-operator (for Choice 1), we show in figure 7 the solutioncomponents ψ and ϕ_n for case = 4 on a 64-grid and a graph of $\theta_{2,j,2}$ (see (6.3a2)).

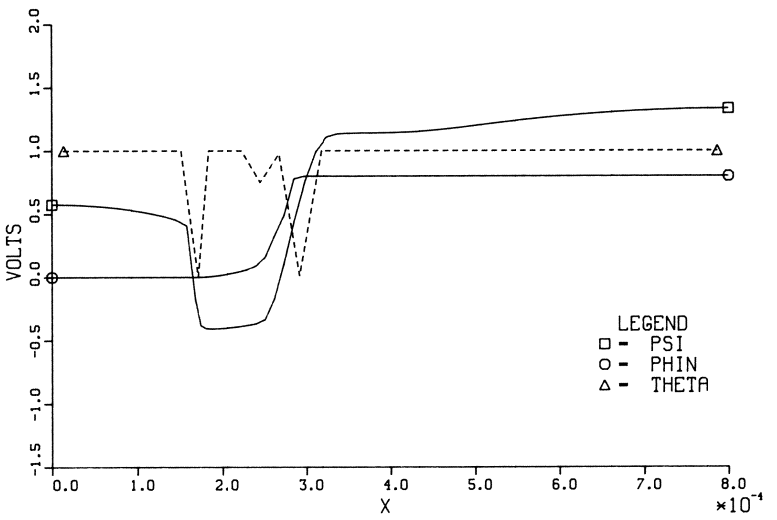

FIGURE 7. The components ψ and ϕ_n of the solution for case = 4 and the corresponding θ.

We observe the typical behaviour that $\theta_{2,j,2}$ equals 1 almost everywhere, except for some isolated points.

We conclude this section with some figures which show the solutions of our problem for all cases. Figure 8 shows the electrostatic potential ψ as computed on a grid of 16 boxes, the figures 9-11 show ψ, ϕ_n and ϕ_p as computed on a grid of 128 boxes. Comparison of figure 8 with figure 9 shows that already on a coarse grid the solution makes sense, which is an indication for the usability of BOX-FMG.

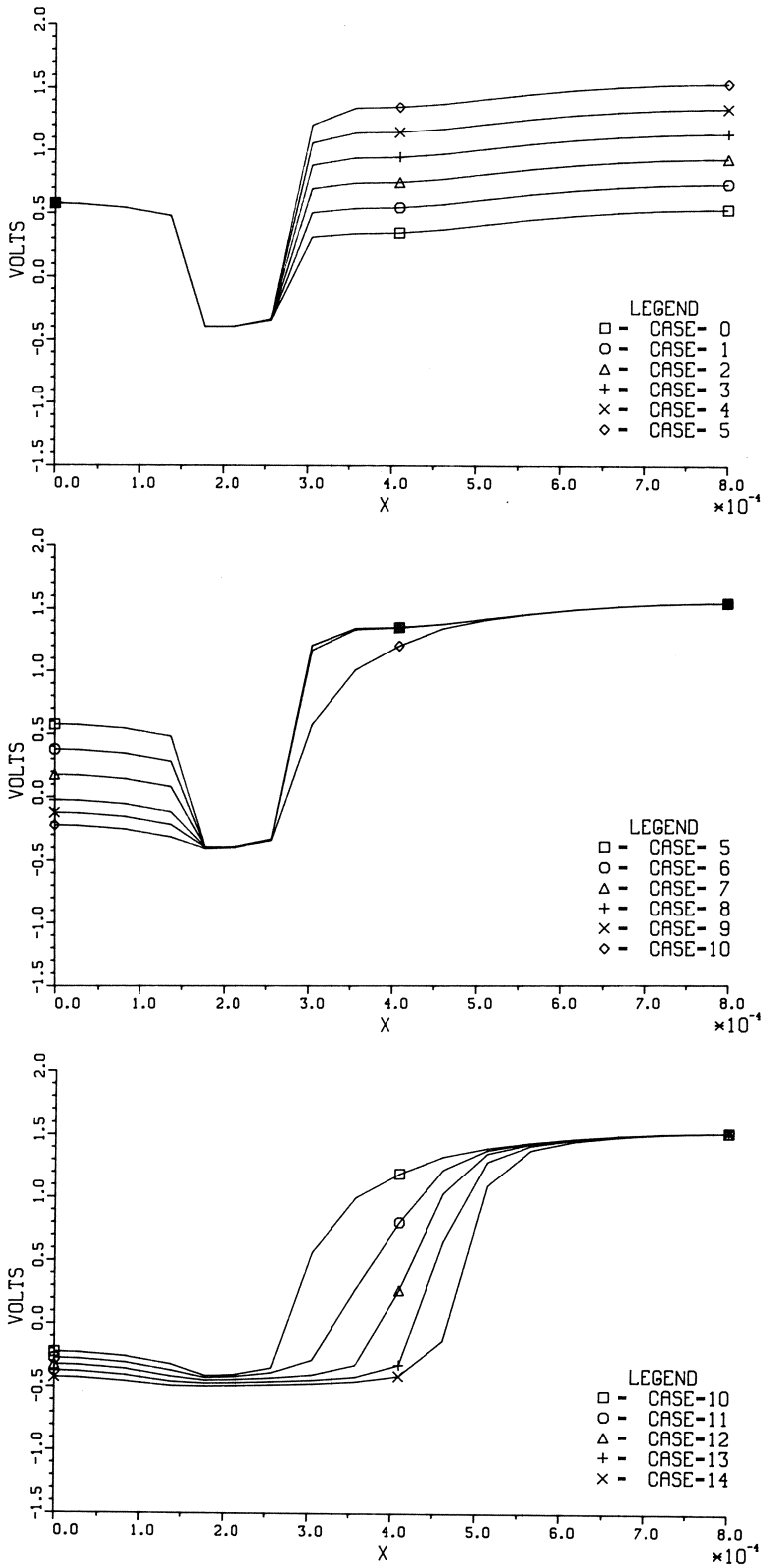

FIGURE 8. The electrostatic potential ψ on a 16-grid.

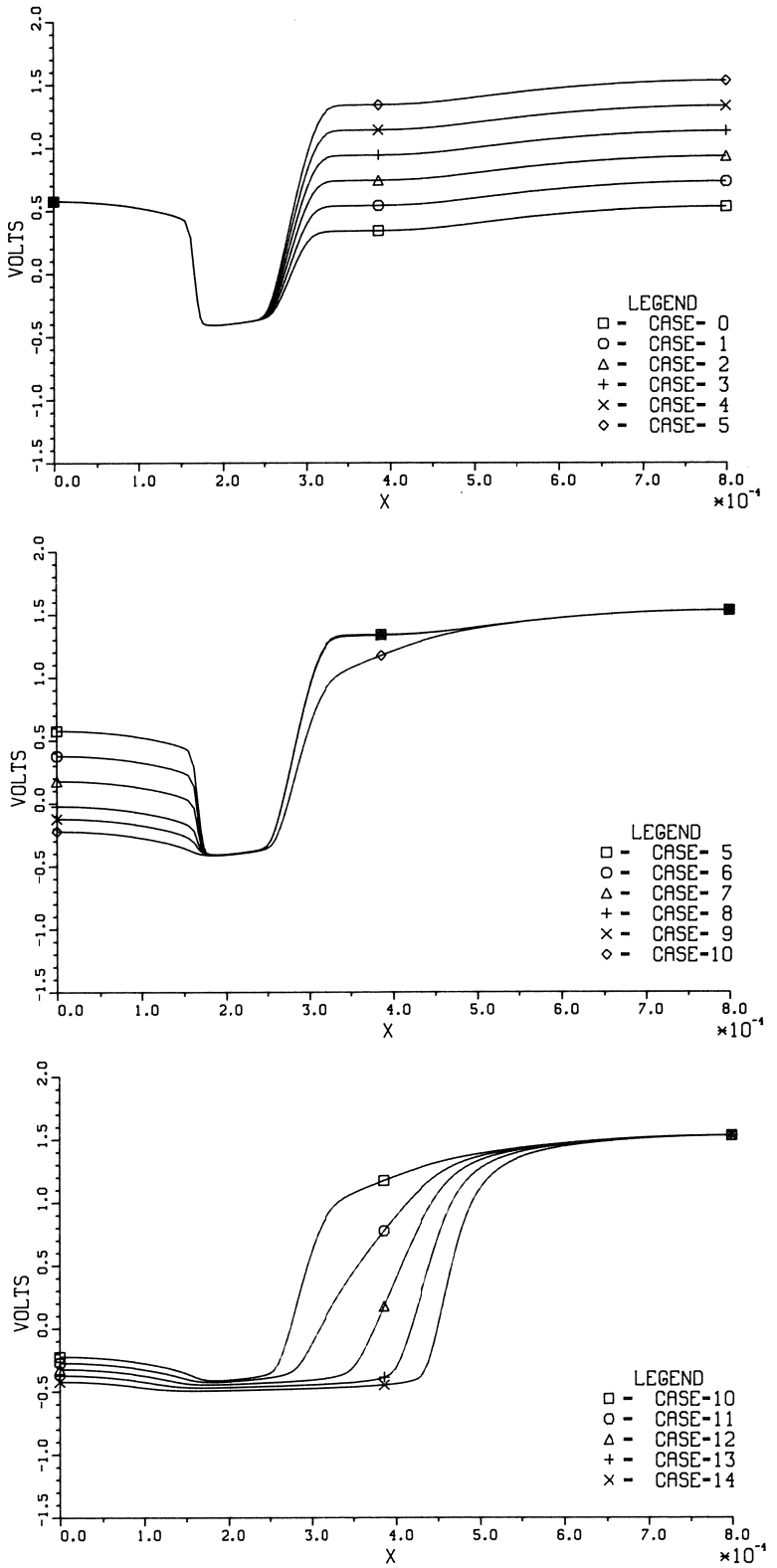

FIGURE 9. The electrostatic potential ψ on a 128-grid.

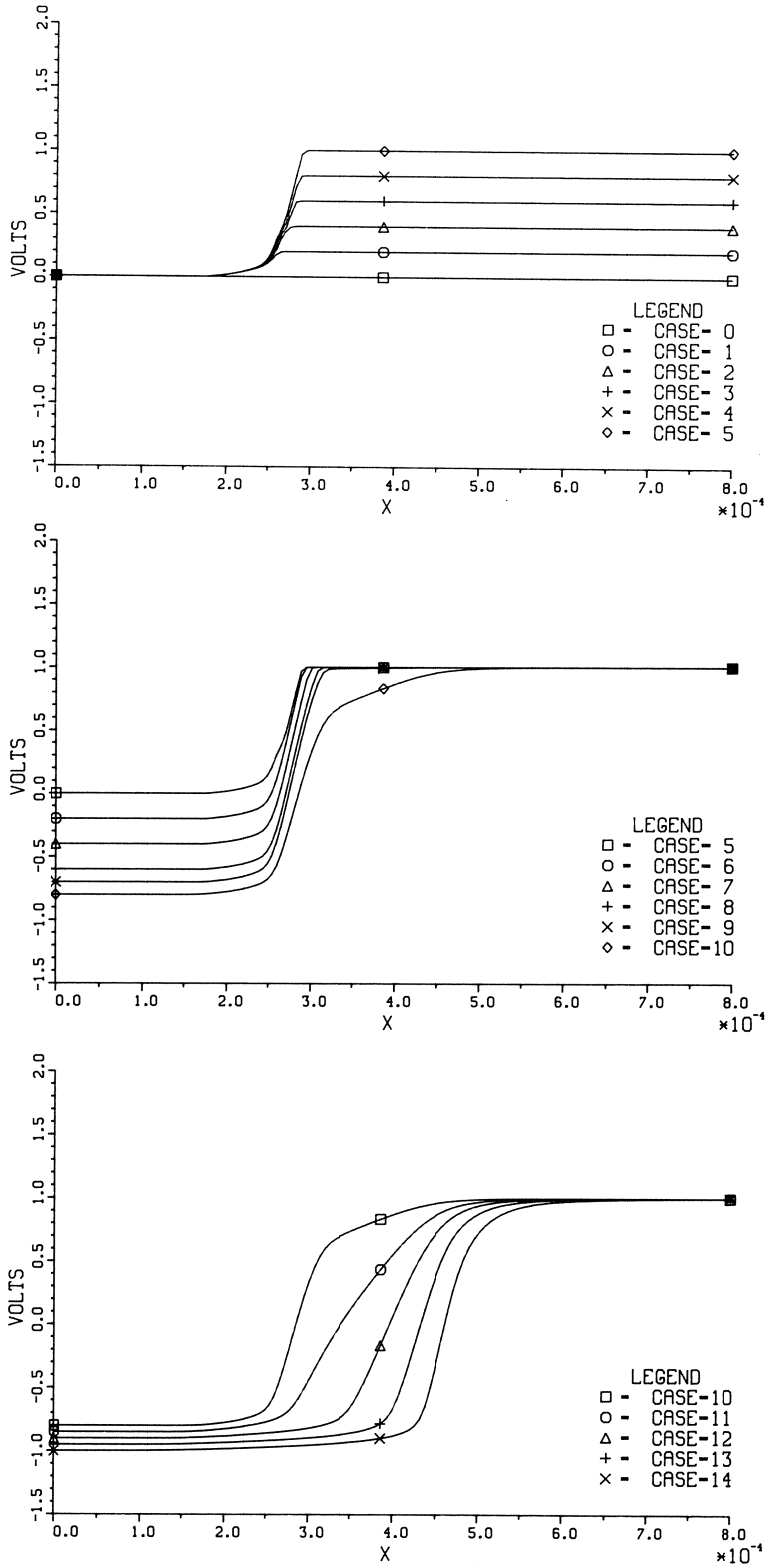

FIGURE 10. The electron quasi-Fermi potential ϕ_n on a 128-grid.

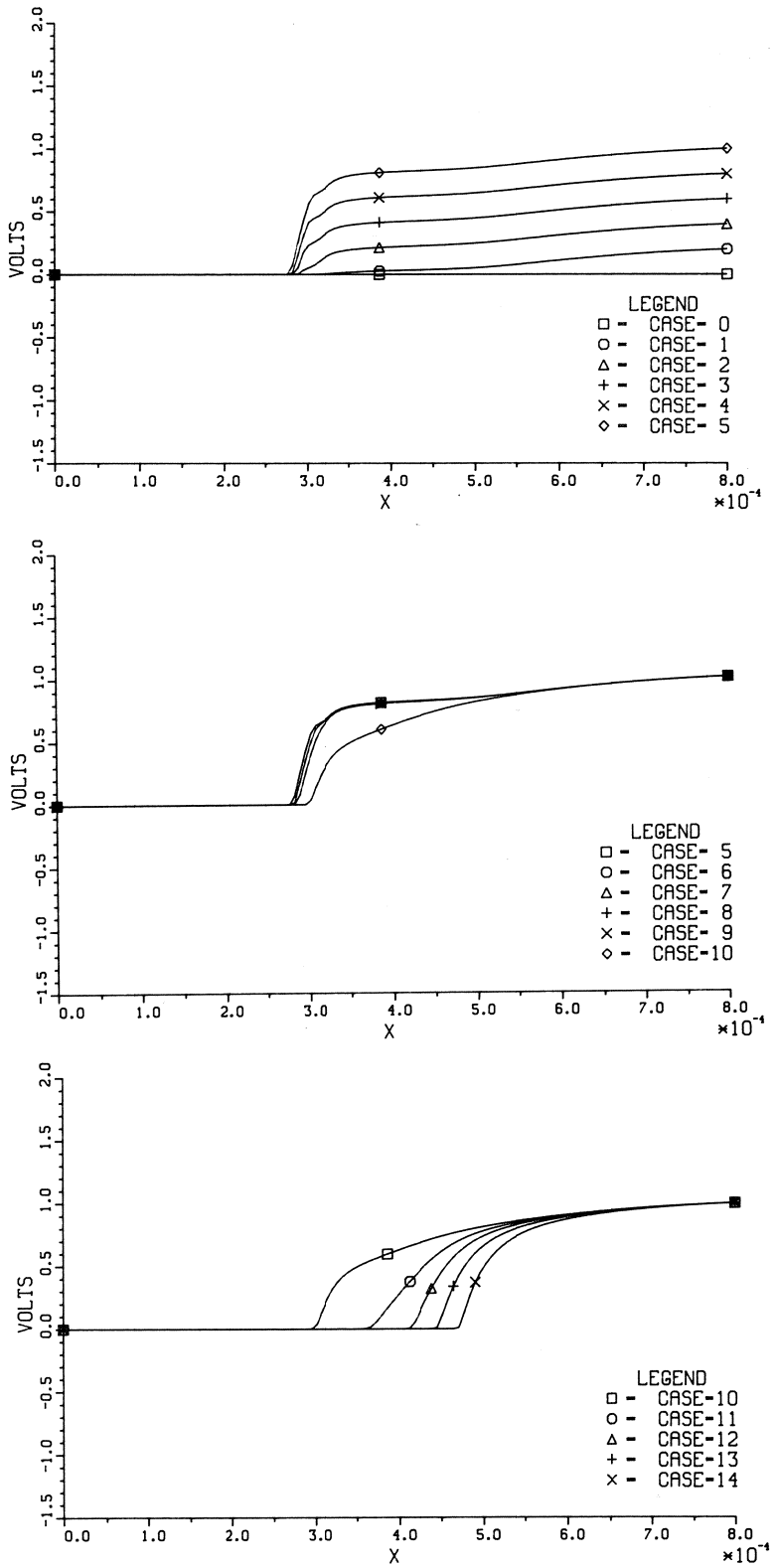

FIGURE 11. The hole quasi-Fermi potential ϕ_p on a 128-grid.

8. Conclusions

We find, by deriving explicit expressions for the entries of the Jacobian, that the linearization of the Scharfetter-Gummel discretization scheme contains a weak spot. When applying Full Multigrid followed by FAS/NMGM-iterations to our 1-D transistorproblem, we find a serious lack of robustness which is explained by the strong nonlinearity of the discretized problem. This difficulty is met by adaptation of the coarse grid correction, which looks equally applicable for the more-dimensional case. A proper choice of the coarse grid solutions is of importance too, e.g. the full weigthing approximation is not satisfactory. Furnished with the improvements as proposed, we obtain a robust multigrid algorithm with a convergence which is independent of the meshsize. Already after application of Full Multigrid (with only one FAS-sweep at each level) we obtain fairly accurate approximations of the discrete solutions.

Acknowledgements

The author wishes to thank Dr. P.W. Hemker and Prof.Dr. P. Wesseling for their useful comments, and Ms. M. Middelberg for typing the manuscript.

References

[1] Bank, R.E., Jerome, J.W. and Rose, D.J. (1982). *Analytical and numerical aspects of semiconductor device modelling.* Computing Methods in Applied Sciences and Engineering, R. Glowinski and J.L. Lions, eds., North-Holland, Amsterdam, pp. 593-597.

[2] Bank, R.E., Mittelmann, H.D. (1986). *Continuation and Multi-Grid for nonlinear elliptic systems.* Multigrid Methods II, W. Hackbusch and U. Trottenberg, eds., Springer Verlag, pp. 23-37.

[3] Brandt, A. (1981). *Guide to multigrid development.* Lecture Notes in Mathematics 960, W. Hackbusch and U. Trottenberg, eds., Springer-Verlag, Berlin, pp. 220-312.

[4] Gaur, S.P. and Brandt, A. (1977). *Numerical solution of semiconductor transport equations in two dimensions by multi-grid method.* Advances in Computer Methods for Partial Different Equations II, R. Vichnevetsky, ed., pp. 327-329.

[5] Hackbusch, W. (1985). *Multi-grid methods and applications.* Springer Series in Computational Mathematics 4, Springer Verlag, Berlin.

[6] Hackbusch, W., Reusken., A. (1988). *On global multigrid convergence for nonlinear problems.* Preprint 503, Dept. of Mathematics, University of Utrecht, the Netherlands. To appear in Robust Multigrid Methods, W. Hackbusch, ed., Vieweg Verlag, Braunschweig

[7] Hemker, P.W. (1988). *A nonlinear multigrid method for one-dimensional semiconductor device simulation: the diode.* To appear: Report NM-R89.., Dept. of Numerical Mathematics, Centre for Mathematics and Computer Science, P.O. Box 4079, Amsterdam.

[8] Polak, S.J., Den Heijer, C., Schilders, W.H.A. and Markowich, P.A. (1987). *Semiconductor device modelling from the numerical point of view.* Int. J. Numer. Math. Engineering 24, pp. 763-838.

[9] Shieh, A.S.L. (1984). *Solution of coupled systems of PDEs by the transistorized multi-grid method.* Proceedings of a Conference on Numerical solutions of VLSI devices, Boston.

[10] Sommeijer, B.P., Hundsdorfer, W.H., Everaars, C.T.H., van der Houwen, P.J., Verwer, J.G. (1987). *A numerical study of a 1D stationary semiconductor model.* Note NM-8702, Dept. of Numerical Mathematics, Centre for Mathematics and Computer Science, P.O. BOX 4079, Amsterdam.

[11] Young, D.M. (1971). *Iterative solution of large linear systems.* Academic Press, New York and London.